




Recent biomedical applications of bio-sourced materials

Abdelrahman Elbaz¹ · Zhenzhu He¹ · Bingbing Gao¹ · Junjie Chi¹ · Enben Su³ · Dagan Zhang¹ · Songqin Liu⁴ · Hua Xu¹ · Hong Liu¹ · Zhongze Gu^{1,2} 

Received: 15 December 2017 / Accepted: 5 January 2018 / Published online: 26 February 2018
© Zhejiang University Press 2018

Abstract

Natural anisotropic nanostructures occurring in several organisms have gained more and more attention because of their obvious advantages in sensitivity, stability, security, miniaturization, portability, online use, and remote monitoring. Due to the development of research on nature-inspired bionic structures and the demand for highly efficient, low-cost microfabrication techniques, an understanding of and the ability to replicate the mechanism of structural coloration have become increasingly significant. These sophisticated structures have many unique functions and are used in many applications. Many sensors have been proposed based on their novel structures and unique optical properties. Several of these bio-inspired sensors have been used for infrared radiation/thermal, pH, and vapor techniques, among others, and have been discussed in detail, with an intense focus on several biomedical applications. However, many applications have yet to be discovered. In this review, we will describe these nanostructured materials based on their sources in nature and various structures, such as layered, hierarchical, and helical structures. In addition, we discuss the functions endowed by these structures, such as superhydrophobicity, adhesion, and high strength, enabling them to be employed in a number of applications in biomedical fields, including cell cultivation, biosensors, and tissue engineering.

Keywords Nature · Bio-sourced · Bio-inspired · Bio-Materials · Biomedical

Introduction

The colors in nature have attracted people's attention since ancient times, from the poems and couplets written by poets, paintings created by artists, ornamental organisms produced by captive breeding, artificial landscapes, and the use of nat-

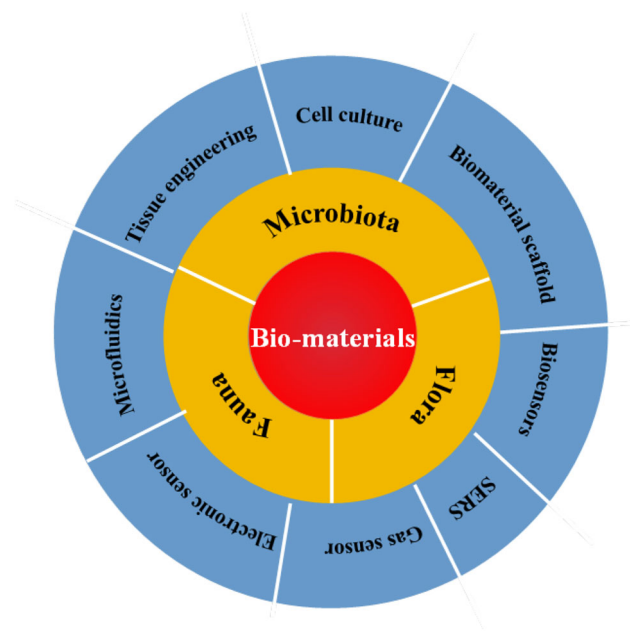
ural raw materials to produce bio-inspired materials, known as bionics [1,2]. Mechanical technology or various other new technology subjects are developed using the structures and functions of organisms.

After reviewing the history of science and technology, many of the major inventions that have affected the progress of human civilization were derived from thinking about bionics [3]; people imitated the structures of plants and animals to create new architectural structures, invented airplanes inspired by the flight of birds, mimicked dolphins to invent submarines, developed robots by imitating the development of human beings and animals, etc. [4]. For example, the imitation of human arithmetic created the computer and the imitation of biological information was used for sensors [5]. All bio-inspired applications are based on the unique structures and specific functions of organisms in nature [6]. The typical biological materials are integrated with functions and corresponding multi scale structures and models. Along with the development of molecular biology and nanotechnology, these bionics have served as a source of inspiration for scientists and engineers to achieve various applications.

Abdelrahman Elbaz and Zhenzhu He have contributed equally to this work and should be considered as co-first authors.

✉ Zhongze Gu
gu@seu.edu.cn

- ¹ State Key Laboratory of Bioelectronics, School of Biological Science and Medical Engineering, Southeast University, Nanjing 210096, China
- ² Laboratory of Environment and Biosafety, Research Institute of Southeast University in Suzhou, Suzhou 215123, China
- ³ Getein Biotech, Inc., No. 9 Bofu Road, Luhe District, Nanjing 211505, Jiangsu, China
- ⁴ Jiangsu Engineering Laboratory of Smart Carbon-Rich Materials and Device, Jiangsu Province Hi-Tech Key Laboratory for Bio-Medical Research, School of Chemistry and Chemical Engineering, Southeast University, Nanjing 211189, China



Scheme 1 An overview of bio-materials and applications in biomedical area

With the generation and development of bionics, thousands of organisms in nature have been studied to examine natural phenomena, explain the mechanism of life, and promote the development of technology for progress in human civilization. The organisms in nature are divided into three main categories, depending on their sources: animals, plants, or microorganisms. These organisms possess a variety of structures, such as layered structures, hierarchical structures, helical structures. These structures are endowed with specific functions, superamphiphobicity, adhesion, and high strength, etc., and have been employed in several applications in biomedical fields, including biosensing, cell cultivation and tissue engineering (Scheme 1).

Organisms in nature

Organisms are classified by taxonomy into specified groups such as the multicellular animals and plants and unicellular microorganisms, such as a protists, bacteria, and Archaea [7,8]. Several organisms have been implemented in many applications based on their typical structures and functional characteristics.

Fauna

The existing known animals are divided into two classes by scientists: invertebrates and vertebrates [9]. Here, we will discuss several typical types of animals that have been studied and applied.

Insects

The compound eye of the mosquito has excellent superhydrophobicity and anti-fogging ability, as droplets do not easily adhere to and remain on the compound eye surface [10–12]. Uniformly arranged hexagonal arrays of nanomas-toidins are present in the ommatidia (Fig. 1A) [12].

Analogous to the compound eye of the mosquito, the moth eye is also composed of ordered micro-/nanostructures [10,13,14]. A very low amount of light has the reflection coefficient of the moth eye, allowing the moth to see in the dark (Fig. 1B) [13].

In addition to the aforementioned micro-mastodons structures, the microstructures of cicada wings are arranged in hexagonal ncp papillae with a spacing of approximately 190 nm (Fig. 1C) [15–17]. Liu et al. developed a new type of imprinting with cicada wings and fabricated nanoarrays that are transferrable to a silicon surface and subsequently showed antireflective properties [15].

Water striders can walk on water, which has attracted the broad attention of researchers.

Water striders stand effortlessly and easily move quickly on water with their specially designed legs (Fig. 1D) [18,19]. The legs of water striders are covered with numerous needle-shaped setae arranged in a similar orientations at the micron scale, with a tilt angle of approximately 20° from the surface [20]. Inspired by the water strider legs, some multiscale structured materials with a superhydrophobic surface have been developed [18,21]. Zhang et al. prepared superhydrophobic coatings on a gold thread to compare their forces and motions on gold wires supported on water surfaces (Fig. 1D) [21].

Creatures living in extreme environments have adapted to live in these environments. Desert plants and animals, the *Stenocara* beetle collects condensed water from fog in the Namib Desert (Fig. 1E) [10,22]. Inspired by the water-collecting mechanism, Wen et al. designed a superhydrophilic bump–superhydrophobic/superoleophilic stainless steel mesh (SBS–SSM) filter using a facile method [Fig. 1E(c)] [23].

In recent years, various functional properties of dragonfly wings have gradually been reported by scholars all over the world, making it an important biological model of bionics [24–29].

Butterflies display various colors that are composed of structured colors and pigments, and the structured color is generated by photonic structures that are formed by arranged and ordered nano-, micron and millimeter wing scales [30, 31]. Figure 2A shows a typical image of *Morpho didius*. The dorsal surface of the wings is divided into cover scales and ground scales; the two layers display a major structure consisting of ridges connected by crossed ribs [32,33].

In addition to *Morpho didius*, other butterfly species contain important wing structures, including *Morpho peleides*,

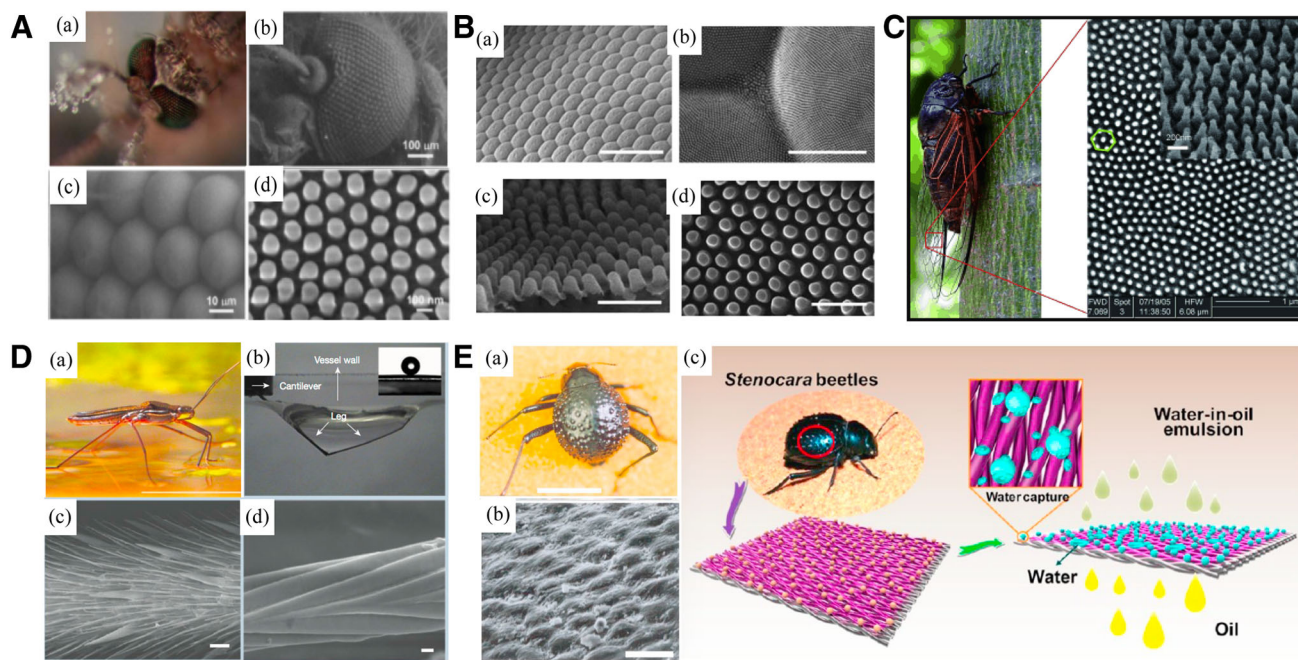


Fig. 1 **A** (a, b) A photo and SEM image of a single mosquito eye. (c, d) A high magnification image of micro-scales (ommatidia). Reproduced with permission from [12], Copyright 2007, Wiley-VCH. **B** The *Attacus atlas* moth eye showing the compound eye structure; Scale bar: (a) 100 mm, (b) 5mm, (c) and (d) 500 nm. Reproduced with permission from [13]. Copyright 2011, The Royal Society of Chemistry. **C** Photograph and SEM image of *Cryptotympana atrata* Fabricius wings. Reproduced with permission from [15], Copyright 2006, Wiley-VCH. **D** The super hydrophobic water strider leg and its application. (a) Photograph of a

water strider. (b) The non-wetting leg of a water strider. (c) SEM image of the leg with an oriented microsetae. (d) A magnification SEM image showing the fine nanoscale grooved structures on a seta. Reproduced with permission from [19,20]. Copyright 2003, 2004, Springer Nature. **E** (a) The water-capturing surface of the fused overwings (elytra) of the desert beetle *Stenocara* sp. (b) Scanning electron micro-graph of the textured surface of the depressed areas. (c) Schematic Illustration of the Preparation of SBS-SSM. Reproduced with permission from [22,23]. Copyright 2001, Springer Nature, 2016 American Chemical Society

Morpho menelaus, *Morpho rhetenor*, *Morpho sulkowskyi*. However, only minor differences are observed between the wing structures of butterflies in the various subgenera [33]; Shin et al. combined the directional deposition method and utilized a silica microspheres base layer and a dielectric multilayer structure to produce oriented sedimentary assemblage (Fig. 2B) [30].

Morpho aega wings display a micro-pattern that comprises groove microstructures, and droplets tend to slide along the groove easier, rather than in the perpendicular direction (Fig. 2C) [34]. Based on this phenomenon, Jiang et al. displayed the droplets directional slide on the superhydrophobic wings of the blue *Morpho* butterfly [35].

Butterfly wings are iridescent, and they have high gas-responsive selectivity. Hence, Potyrailo and his coworkers developed a highly selective sensors using *Morpho* wings that were inspired by the natural sensing design (Fig. 2D) [36–38].

The color of the butterfly wings is largely related to the photonic crystal. Thus, natural hierarchical photonic structures have been used to fabricate various sensors, such as thermoresponsive sensors [39,40]. Xu et al. reported a simple

method for producing an intelligent sensor that exhibited high performance and tunable color as the temperature changed (Fig. 2E) [41].

Likewise, the three-dimensional ordered nanostructures of *Morpho* butterfly wings have been used to fabricate infrared (IR) sensors (Fig. 2F) [42,43].

In addition to sensors, the highly ordered structures and large specific surface areas of butterfly wings have also been used to generate surface-enhanced Raman scattering (SERS) substrates [44,45]. Zhang et al. reported the development of a stable and facile SERS substrate to detect an important tumor marker, carcinoembryonic antigen (CEA) (Fig. 2G) [46].

Reptiles

As a common reptile in nature, geckos can walk on smooth walls and can even adhere to the ceiling and crawl quickly [45,47]. These characteristics are caused by the combination of the size effect of the micro-/nanosetae and sophisticated motion control geckos, using the adductor and valgus of foot hallux that ultimately enable it to stand and walk on walls and ceilings [Fig. 3A(a)] [48]. Jiang et al. first used the highly

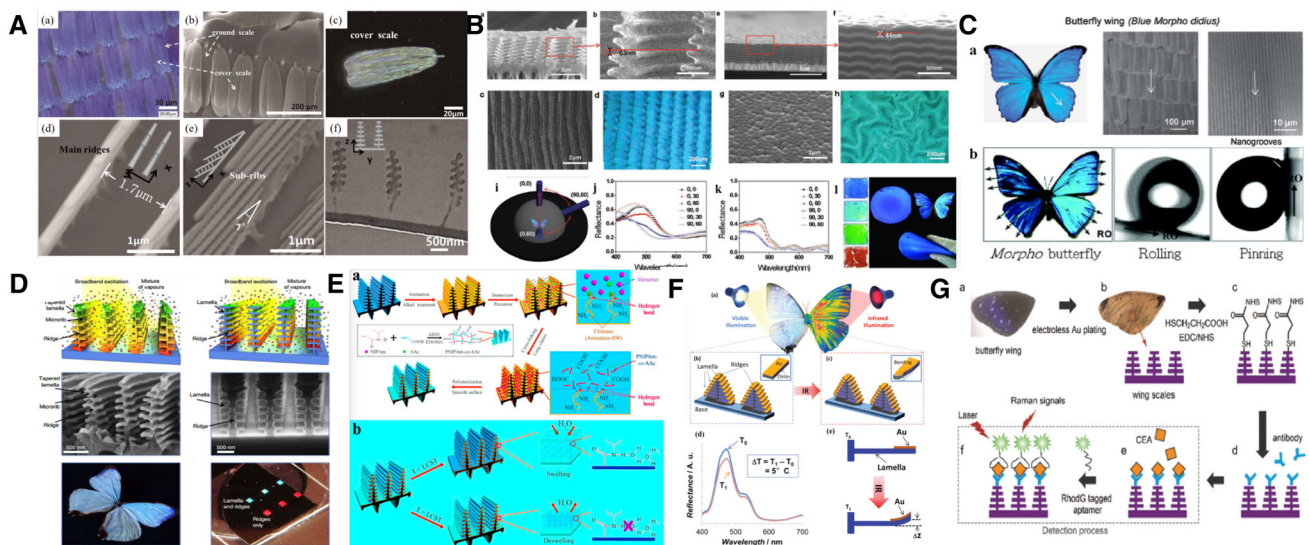


Fig. 2 **A** (a) Optical images of the scales. (b) The cover scale and the ground scale. (c) Optical image of a single cover scale. (d) SEM image of a cover scale from the top view. (e) SEM image of the ground scale. (f) TEM image of the ground scale. Reproduced with permission from [32]. Copyright 2014, Royal Society of Chemistry. **B** Structural comparison between butterflies (a–d) and fabricated films (e–h). (i–k) Analysis of optical performance. (l) Images of fabricated films of various colors ranging from deep blue through green to coppery red that were achieved by controlling the layer thicknesses. Reproduced with permission from [30]. Copyright 2012, Wiley-VCH. **C** Directional adhesion on super hydrophobic butterfly wings. (a) SEM images of the blue butterfly *M. aega*. (b) The black arrows denote the radial outward (RO) direction away from the center axis of the body. The droplet easily rolls along the RO direction when the wing is tilted downwards. Repro-

duced with permission from [34,35]. Copyright 2006, 2012, Royal Society of Chemistry. **D** Design and fabrication of highly selective vapor sensors inspired by Morpho butterflies. Reproduced with permission from [36]. Copyright 2015, Springer Nature. **E** (a) Overall synthesis of thermoresponsive PCs from Morpho BWs. (b) Mechanism underlying the temperature responsiveness of PNIPAM-co-AAc-PCs. Reproduced with permission from [41]. Copyright 2015, American Chemical Society. **F** (a–c) Schematic illustration showing the IR response of the selectively modified butterfly wing structures. (d, e) IR response for Au-modified butterfly wings (Au thickness is ca. 50 nm). Reproduced with permission from [43]. Copyright 2014, Wiley-VCH. **G** Schematic of CEA detection using Au butterfly wings. Reproduced with permission from [46]. Copyright 2017, Royal Society of Chemistry

sensitive the MEMS balance system to study the adhesion of the superhydrophobic gecko foot [Fig. 3A(b)] [49].

Snakes do not have limbs but can move smoothly like flowing water, and the weight of a snake is evenly distributed along its body, allowing it to move in barren or marshy environments [50,51]. The spine extends from a series of similar bony vertebrae from the occipital portion of the skull to the tip of the tail, and the continuous insertion of the two bones of the vertebral body is connected by the intervertebral disk [52]. These joints are deflected at a small angle around the axis in all directions. In addition, these joints make the snake easily bend in 360°, as shown in Fig. 3B [50].

With natural evolution, some organisms with biological composite structures have adapted to resist penetration, such as tortoise shells. In general, they contain organic and inorganic components in complex mixtures that are hierarchically organized at the nano-, micro-, and mesoscales [53]. A number of studies on the structural and mechanical responses of different biological composites have been extensively reported in the literature. For example, the skin tissues and deformation behaviors of crabs and lobsters have been studied by John et al. [54]. Turtles are reptiles of the order

Testudines and are characterized by a special bony or cartilaginous shell that develops from their ribs and acts as a shield [55]. Rhee et al. studied the materials, geometric features, and the correlation between the multiscale/microstructures and the structural characteristics of tortoise shells (Fig. 3C).

Crocodiles are wild animals with scientific research value, ecological value, and high economic value [56–58]. The fragmented skin on the crocodile head provides an appropriate example of skin debris research, similar to the scales of snakes, lizards and fishes that can protect themselves (Fig. 3D) [58,59].

Marine life

Nacre is the main component of an armored system of shells used by some animals to protect themselves from predators and other mechanical forces that displays strong, stiff, and tough properties (Fig. 4A) [60–62].

In the sea, mussels are a mixed underwater fouling organism that attach to almost all natural or artificial organic/inorganic matrices under humid conditions. The presence of 3,4-dihydroxy-L-phenylalanine (DOPA), a cate-

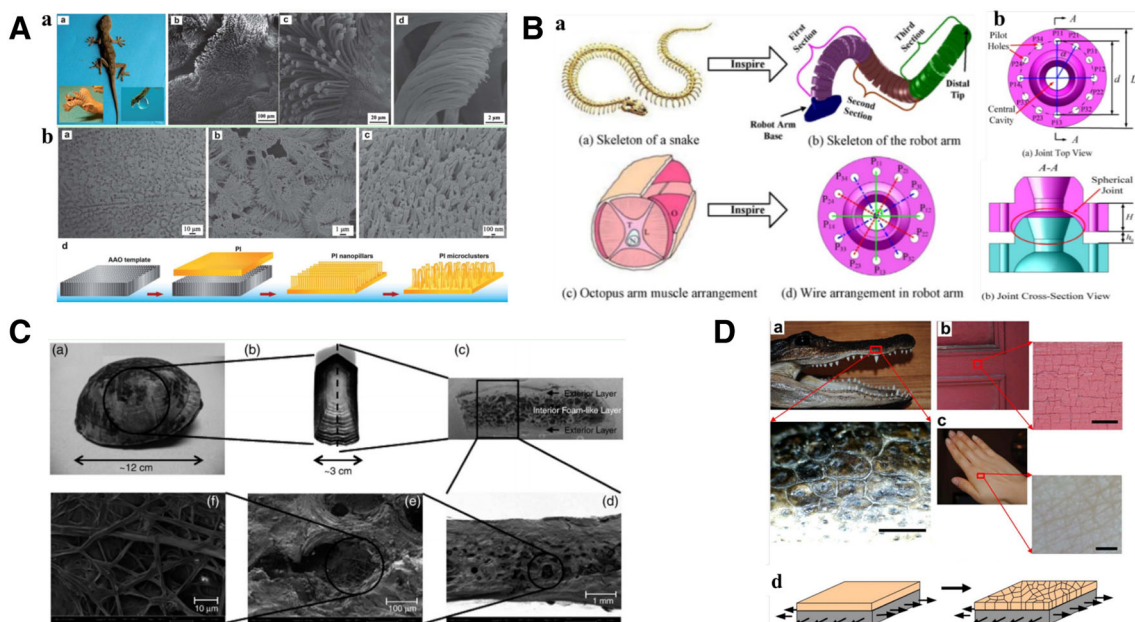


Fig. 3 **A** (a) Photo and SEM images of gecko feet. (b) SEM images of gecko-inspired polyimide films at different magnifications showing the gecko-like multiscale structures with densely packed microclusters composed of nanopillars, and a schematic representation of the formation of multiscale structured polyimide (PI) materials using AAO as templates. Reproduced with permission from [49]. Copyright 2012, The Royal Society of Chemistry. **B** (a) Wire-driven robot arm inspired by the snake skeleton and octopus arm muscle arrangement. (b) Top view of the joint and cross-section view of the wire-driven robot. Reproduced with permission from [50]. Copyright 2013, SAGE Publications Ltd. **C** Multiscale hierarchy and structure of the turtle shell. (a) Morphology of the turtle shell carapace. (b) A costal scute showing the successive growth pattern. (c) A cross-sectional view of the carapace showing

composite layers. (d) An SEM micrograph of a fracture surface. (e) An SEM micrograph of a cell structure, and (f) An SEM micrograph of the fibrous structure inside the cell. Reproduced with permission from [55]. Copyright 2009, Elsevier. **D** The observed skin fragmentation patterns in animals, paint and skin. (a) Snapshot of a crocodile head. Bottom: high magnification image of skin fragmentation in the form of scales on a crocodile head surface (the crocodile is small, with an eye to nose distance of 90 mm). Scale bar: 4 mm. (b) Skin fragmentation observed on the surface of painted door. Scale bar: 1 cm. (c) Skin crumpling observed on the back of a hand. Scale bar: 2 mm. (d) Schematic of the mechanical model used to model skin fragmentation under deformation stress. Reproduced with permission from [58]. Copyright 2014, Nature Publishing Group

chol amino acid secreted by mussel mucin, is responsible for strong underwater bonding [Fig. 4C(a)] [63–65].

Underwater animals (such as carp and shark) swim freely because of the specific structure of their surface. The surfaces of superoleophobic fish originate from the micro-/nanometer water-phase hierarchical structures [66,67]. For example, sharks have squamous scales, including rectangular basins embedded in the skin and tiny thorns or bristles that are raised from the surface [68]. Barthelat et al. investigated the structure and mechanism of a single bony fish (Ctenoid), the striped bass *Morone saxatilis* (Fig. 4D) [69].

In nature, corals have a special dendritic structure that has attracted rapidly increasing research interest worldwide. Corals develop in the form of microcrystalline calcite aggregates [70]. Tao et al. prepared a series of composite electrode materials by depositing conducting polymers on a monolithic coral-like porous carbon (MC), as shown in Fig. 4E(a) [71].

Jellyfish is a very beautiful aquatic animal with a shape resembling a transparent umbrella, and the diameter of large jellyfish reaches up to 2 m. The edge of the umbrella body

contains some tentacles, which can be up to 20–30 m in length (Fig. 4F) [72,73].

Other animals

In addition to the above-mentioned animals, many other organisms also exhibit specific structures and exceptional functions. Another common example of a surprising natural color is peacock feathers, which exhibit different colors due to the presence of complex, tiny, two-dimensional photonic crystal structures [10,74]. Zhang et al. selected peacock feathers as the matrix for embedding ZnO nanoparticles using in situ methods [75].

Natural spider silk has superior mechanical properties, particularly its high specific strength (approximately 5 times greater than steel) and excellent flexibility (approximately 10 times greater than aramid) and toughness (the highest of any material) [76–78].

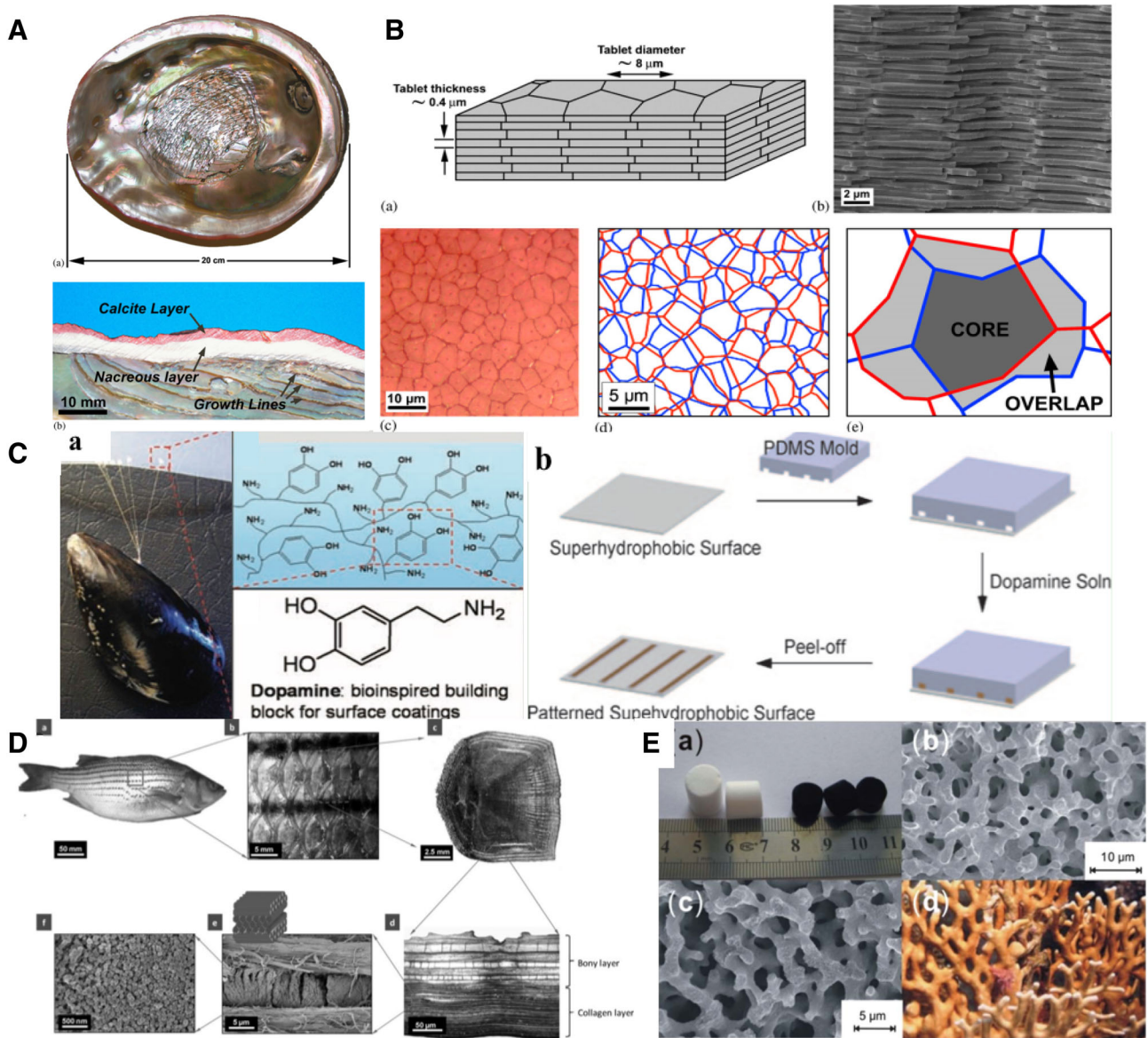


Fig. 4 **A** The multiscale structure of nacre: view of the inner nacreous layer of a red abalone shell. **B** Nacre at the mesoscale: **(a)** schematic of the tablet arrangement in nacre; **(b)** SEM image of a fracture surface in nacre; **(c)** top view of the tablet tiling in nacre; **(d)** reconstitution of the arrangement of the tablets from one layer to the next; **(e)** core and overlap areas in the tablet arrangements. Reproduced with permission from [62]. Copyright 2006, Elsevier. **B** Experimental tensile stress–strain curve for nacre and **(b)** associated deformation modes. **(c)** Experimental shear stress–strain curve for nacre and **(d)** associated deformation modes. Reproduced with permission from [62]. Copyright 2006, Elsevier. **C** Mussel-inspired super hydrophobic surface modification. **(a)** Photograph of a mussel attached to commercial PTFE and the amino acid composition of proteins found near the plaque-substrate interface.

(b) Schematic showing the method used to prepare a polydopamine-patterned super hydrophobic surface. Reproduced with permission from [64]. Copyright 2007, American Association for the Advancement of Science. **D** The hierarchical structure of a teleost fish scale from the striped bass *M. saxatilis*. **(a)** Images of the whole fish, **(b)** staggered multiple scales, **(c)** an individual scale, **(d)** a cross section of a scale, **(e)** the cross-ply collagen structure, and **(f)** collagen fibrils. Reproduced with permission from [69]. Copyright 2012, Wiley-VCH. **E** **(a)** Optical image of the monoliths of the silica template (ST) and the as-prepared carbon materials (MC). **(b, c)** SEM images of ST and MC. **(d)** Optical image of coral. Reproduced with permission from [71]. Copyright 2013, The Royal Society of Chemistry

Flora

Lotus leaves are the most common hydrophobic surfaces in nature and have been studied for many years (Fig. 5A) [11,79,80]. In 1997, Barthlott and colleagues were the first to reveal that the lotus leaf comprises a micro-/nanoscale structure consisting of randomly oriented shepherd epidermal cells covered by a hydrophobic wax [79]. Liu et al. combined the self-cleaning effect of lotus leaves, the structure of nacre and the adhesive property of mussel adhesive protein to fabricate graphene composite paper with the integration of these characteristics [80].

In nature, other species with superhydrophobicity have also been observed and studied. For example, rose petals show a high water contact angle (CA) and a water-adhesive property [11,81]. A periodic array of microarrays and nanoscale cuticular folds on top of each micropapilla was observed on the surface of rose petals (Fig. 5A). Feng et al. used the solvent evaporation-driven nanoimprint pattern transfer process to replicate the micro-/nanostructures of rose petals [82]. Lai et al. used simple electrochemical methods to change the diameter and length of nanotubes and reported the development of nanostructured superhydrophobic TiO₂ films with adjustable surface adhesion properties [83].

In addition to the superhydrophobicity of the lotus leaf and rose petals, rice leaf is another natural species that displays anisotropic wetting [10,84]. The rice leaf also exhibits a hierarchical structure with waxy nanobumps, but the quasi-one-dimensional arrangement of microcapsules leads to anisotropic wettability [Fig. 5B(a)] [84]. Wu et al. prepared oriented poly (vinyl butyral) nanofiber arrays using an oriented electrospinning technique [Fig. 5B(b)] [85]. Kang et al. developed three types of anisotropic micro-channel arrays with various shapes, such as prisms, rectangles and overhang structures, using UV-assisted micro-molding techniques, followed by octafluorocyclobutane surface modification [86].

Recently, uni-directional liquid spreading on the peristome of *Nepenthes alata* has been observed, which is mainly derived from its unique superhydrophilic layered structure and micro-cavities with curved edges and a sharp wedge angle (Fig. 5C) [87,88]. A novel bio-inspired uni-directional liquid spreading surface was proposed and fabricated using a two-step oblique UV exposure lithography technique inspired by *N. alata* by Chen et al. [89].

Natural bamboo (*Phyllostachys pubescens*) is an eco-friendly, widely distributed and versatile plant in nature. In recent years, more and more interest and research have been devoted to the use of bamboo as an eco-friendly material for a wide range of engineering and civil construction applications, including scaffolds, fiber-reinforced composites and bridges [60,90]. Bamboo has been used as a raw material for the isolation of biologically active substances, such as two C,C-hexosyl proteins, O-hexosyl-O-deoxyhexosyl sar-

cosine and 6-C-glucose alkaline starch protein, which have high antioxidant, antibacterial, and melanin inhibitory and antiallergic activities [91]. Gao et al. used a simple and extensible combination of hydrothermal carbonization, activation, and vacuum annealing to successfully fabricate a novel bio-inspired honeycomb layered nanocomposite (BHNC) using bamboo-based industrial by-products as model carbon precursors (Fig. 5D) [92].

Microbiota

Microorganisms comprise a wide variety of biological groups, including bacteria, viruses, fungi, some small protozoa, microscopic algae, etc. [93]. The industrial applications of microorganisms include the food industry, pharmaceutical industry, metallurgy, mining, oil, leather, light chemical industry, and other industries [94–97]. Through a genomic study of *Bacillus subtilis*, a series of genes related to the production of antibiotics and important industrial enzymes was identified [98]. *Lactobacillus* is an important microecological regulator that has been used in the food fermentation process; genomics research of this organism will help researchers identify the key functional genes and then transform the strain to make it more suitable for industrial production processes [99].

A large number of microorganisms have the ability to oxidize and decompose complex organic matter and certain inorganic substances, and convert these substances into simple substances, or convert toxic substances into non-toxic substances [96,100]. Xu et al. investigated the feasibility of using a bio-electrochemical system integrated with a capacitor deionization-microbial electrolytic desalination tank (MCDC) to treat the actual shale gas-produced water [101].

Many organisms provide inorganic materials intracellularly or extracellularly [102–104]. For example, unicellular organisms such as magnetotactic bacteria produce magnetite nanoparticles and [102] diatoms produce synthetic siliceous materials [103]. Gadd et al. studied the effects of the ureolytic fungi *Neurospora crassa*, *Pestalotiopsis* sp. and *Myrothecium gramineum* to generate nanoscale copper carbonate and examined the roles of fungal extracellular proteins in the formation of this mineral [104].

Microalgae carbon dioxide fixation systems are an environmentally friendly, energy-efficient, and cost-effective method for addressing the problem of global warming, which is mainly caused by the increase in atmospheric carbon dioxide (CO₂) produced by fossil fuel combustion [105,106]. Miyamoto et al. have previously proposed a system for the conversion of algae biomass to H₂ using photosynthetic bacteria [107]. In addition to water treatment applications, microbes can decompose organics to generate energy, which is called a microbial fuel cell (MFC) [108,109].

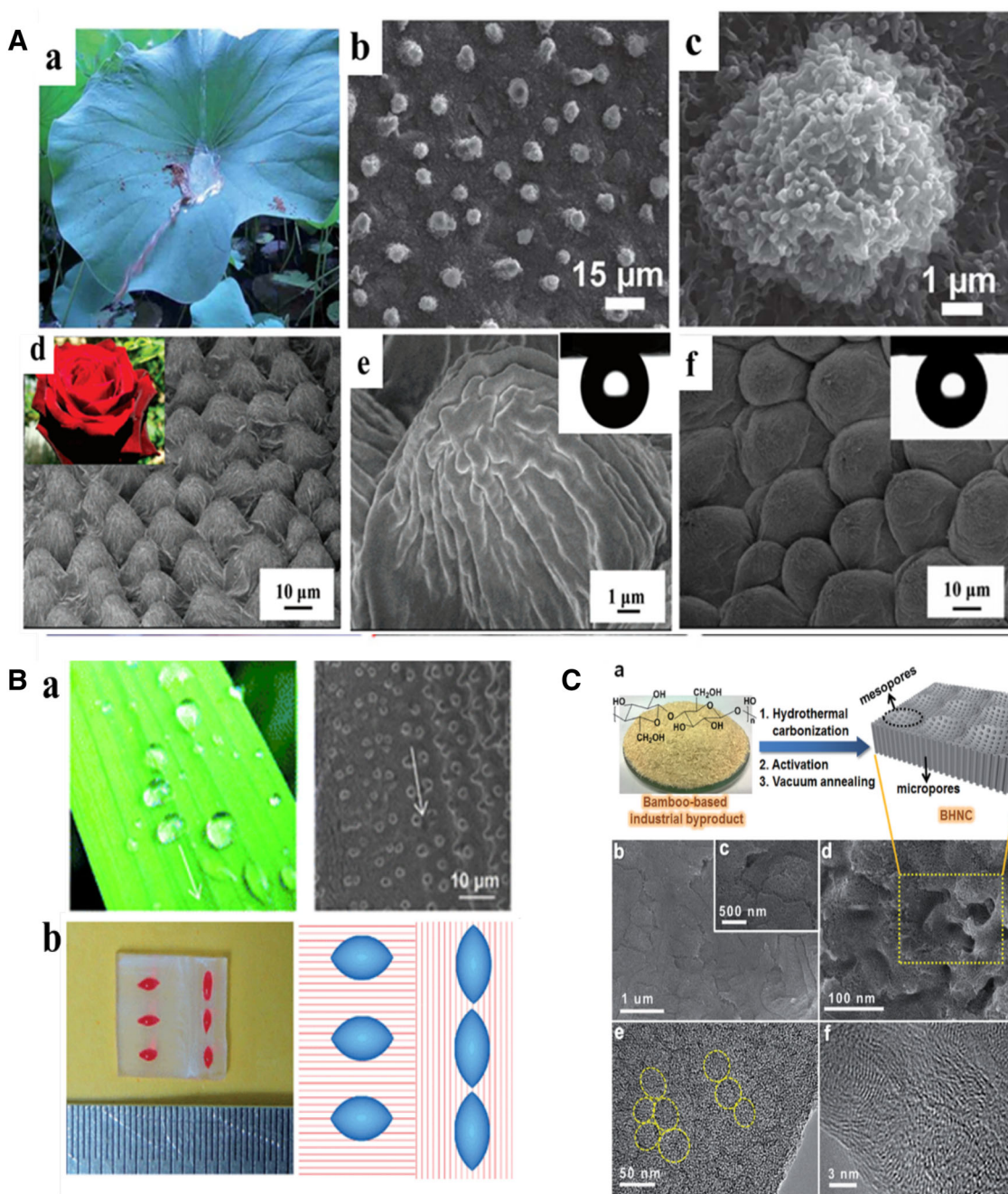


Fig. 5 **A** (a) Photograph and SEM image of a lotus leaf. (b, c) ESEM images of the lotus leaf at different magnification. (d, e) Photograph and SEM images of rose petals. (f) SEM images of the fabricated PS film with the similar petal’s surface structures. Reproduced with permission from [11,80]. Copyright 2011, Elsevier, 2008, American Chemical Society. **B** (a) Digital photos and scanning electron microscope (SEM) images of rice leaves. (b) Digital photograph of a piece of a glass strip that was divided into two sections by vertically oriented nanofiber arrays. Different sections show different wetting anisotropy characteristics in this picture. Reproduced with permission from [84,85]. Copyright 2008, 2012, The Royal Society of Chemistry. **C** (a) Schematic of

procedures used to synthesize the BHNC sample with beehive-like hierarchical nanoporous structures, where the micropores formed on the meso/macropores walls of the interconnected carbon nanosheet frameworks. (b–d) FESEM and (e) TEM images of the beehive-like microstructures of the BHNC sample, and (f) HR-TEM image of the edge of the BHNC. The beehive-like hierarchical nanoporous carbon framework is clearly visible in the structural model shown in (a) and is shown at higher magnifications in (b–d) and highlighted by the yellow rings in (e). Partial graphitization was observed in the distorted lattice fringe image of the BHNC (f). Reproduced with permission from [92]. Copyright 2015, The Royal Society of Chemistry

Applications in biomedical fields

Organisms in nature have evolved many unique structures and excellent functions, which are the source of inspiration for human inventions. With the development of technology, natural, non-toxic, biocompatible and biodegradable natural materials, as well as biomimetic materials, have been widely used in the biomedical field, such as cell cultivation, biosensors and tissue engineering [110,111].

Tissue engineering

Tissue engineering is an emerging discipline that combines cell biology and materials science for the *in vitro* or *in vivo* construction of tissues or organs. The aim is to obtain a small amount of living tissue from the body, use special enzymes or other methods to isolate cells (also known as seed cells) from the tissue culture for *in vitro* expansion, and then mix the expanded cells with good biocompatible, biodegradable and absorbable bio-materials (scaffolds) in the appropriate proportion to allow the cells to adhere to the biomaterial (scaffold) to form a cell–material complex. Next, the compound is implanted into tissue or organ lesions in the body; with the gradual degradation and absorption of bio-materials in the body, the implanted cells proliferate and secrete extracellular matrix in the body and finally form corresponding tissues or organs to achieve the purpose of repairing the wounds and reconstructing functions [112,113]. The three or four elements required for tissue engineering mainly include the isolation of seed cells, production of biological materials, the integration of cells and biological materials, and the integration of implants with the microenvironment in the body. Simultaneously, the development of tissue engineering techniques will also change the traditional medical model and enable further developments in regenerative medicine that will ultimately be used in the clinic.

Cell culture

The primary step in tissue engineering is cell culture. Cell culture *in vitro* requires specific conditions *in vivo* that must mimic physiological conditions in the body, where the medium, the substrate, the culture equipment, etc., influence cell growth and activity. With the development of biological technology, researchers have achieved the transformation from static cultivation to dynamic cultivation, from 2D cultivation to 3D cultivation [114,115]. Compared to static cultivation, dynamic cell cultivation methods display a better interchange of nutrients, energy, gas, and excreted substances. Meanwhile, 3D models are more physiologically relevant than 2D cell cultivation because the 3D models more closely represent the microenvironment, the cell–cell interactions, and the true biological processes *in vivo* and exhibit

a higher degree of similarity to cell morphology and functional differentiation *in vivo*. However, the continuous supply of nutrients is a major challenge in 3D cell culture.

Hydrogels are widely used in three-dimensional fixation and cell culture in basic biological research, biochemical processes, and clinical treatments [115,116]. However, the ability to support cell viability and modulate the cell phenotype in a structurally stable gel remains a challenge as the gel becomes harder and harder as the stiffness increases [115]. Some marine organisms have been shown to exhibit unique microstructures that facilitate molecular transport through their elastic tissues. For example, the skin of blue whales and brain corals exhibit a textured relief such that the skin can absorb a larger number of molecules, including water [115,117]. Inspired by the texture of the grooved skin of marine animals, Lee et al assembled hydrogels that contained computationally optimized micro-sized grooves on the surface (Fig. 6A) [115]. In addition, the gel was designed through a uniaxial freeze-drying process to be a pre-set aligned micro-channel similar to a plant's vascular bundle. The resulting gel showed significantly increased water diffusivity with less variation in gel stiffness, but only when the microgrooves and micro-channels were aligned together. When microgrooves and micro-channels were not aligned, no significant enhancement in rehydration was achieved. The design of this material greatly enhanced the viability and neural differentiation of stem cells and the formation of 3D neural networks in the gel.

In addition, most plants have anisotropic, aligned vascular bundles in their stems that enable the roots to supply all parts of the plant body with the absorbed water and nutrients. The vein of a leaf is considered an optimal transport system. Mesophyll cells are divided into small areas by fine veins called pellets. The transpiration of water in different parts of the leaves fluctuates with time, and thus, the transport of moisture in the veins also fluctuates [118]. However, due to the existence of multiple paths in the vein network and dimples on the vessel wall, the pressure field and nutrient concentration in the pores in which the mesophyll cells are located are nearly uniform. Therefore, inspired by this structure, Liu et al. designed a novel cell culture chambers to achieve a stable and homogeneous microenvironment [119]. The device consisted of a new micro-channel system that mimicked the vessels in the veins to transport the medium, and the cell culture chamber mimicked the areole and included microgaps that mimicked the pits (Fig. 6B). The effects of the areole and pits on the cell culture chamber flow field were discussed. The bio-inspired microfluidic devices were robust platforms that provided fluid-like microenvironments *in vivo*.

In addition to natural bio-materials, bio-inspired materials have great prospects in cell culture. Our group has a long-standing commitment to developing bio-inspired materials for biomedical applications, such as photonic crystals. Cell

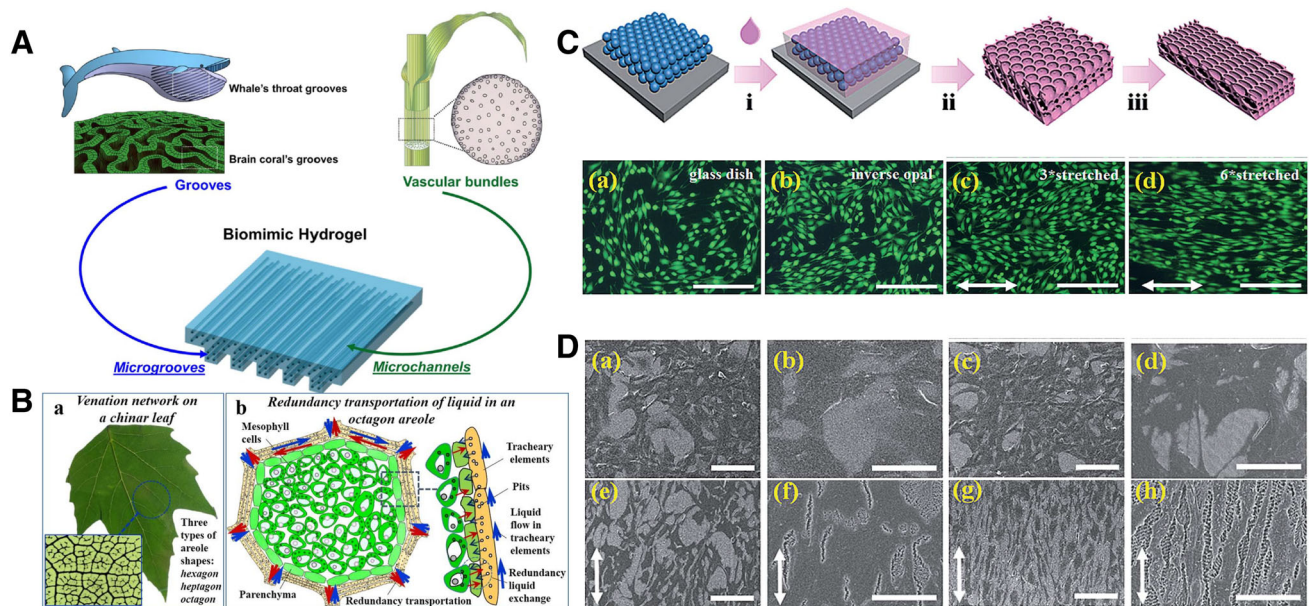


Fig. 6 **A** Schematic describing a strategy for controlling hydrogel permeability by recapitulating the microgrooves of marine organisms (e.g., blue whale and brain coral) and microvascular bundles in plant stems. Reproduced with permission from [115]. Copyright 2015, Nature Publishing Group. **B** The transport of liquid in an octagonal areole. **(a)** The areoles on a chinar leaf, which mainly have three kinds of shapes, i.e., hexagon, heptagon and octagon. **(b)** The structure of an octagonal areole and the transport of liquid in it. Reproduced with permission from [119]. Copyright 2017, The Royal Society of Chemistry. **C** Schematic diagram of the preparation of the stretched inverse opal films. Fluorescence microscopy images of NIH-3T3 cells cultured on different substrates after 48 hours: **(a)** on a glass dish, **(b)** on an unstretched

inverse opal substrate, **(c)** on three-fold and six-fold stretched inverse opal substrates **(d)** Scale bars represent 200 μm . Double-sided inverse arrows indicate the direction of stretching. Reproduced with permission from [120]. Copyright 2014, The Royal Society of Chemistry. **D** SEM images of tendon fibroblasts cultured on different portions of one substrate: **(a)** on an unstretched portion; **(b)** on a 3-fold stretched portion; **(c)** on a 6-fold stretched portion and a 12-fold stretched portion; and **(d)** on a 12-fold stretched portion. **(e–h)** High magnification images of the images shown in **a–d**. Black arrows indicate the cell orientation. White arrows indicate the direction of stretching. Scale bars represent 200 μm in **a–d** and 20 μm in **e–h**. Reproduced with permission from [121]. Copyright 2015, American Chemical Society

adhesion and alignment are two important considerations in tissue engineering applications as they regulate subsequent cellular proliferation and differentiation procedures. Thus, Gu et al. proposed a bio-inspired inverse opal substrate with an adjustable nanoscale patterned structure for regulating cell adhesion and alignment, which was rooted in photonic crystals inspired by opals (Fig. 6C) [120]. Substrates with different pattern orientations were achieved by tailoring the amount of stretch applied to the polymer inverse opal film. Cells cultured on these substrates showed an adjustable morphology and alignment. Meanwhile, soft hydrogels that had poor plasticity and were difficult to cast into a patterned structure were used to infiltrate the inverse opal structure. Cell adhesion rates, cell morphology, and alignment were modulated by these hybridized substrates. In addition, the authors established a gradient of cell orientations using a simple stretched anti-opal substrate (Fig. 6D) [121]. Rendon fibroblasts grown on a stretched inverse opal gradient exhibit an arrangement corresponding to the elongation gradient of the substrate. This “random alignment” of cell gradients reproduced the insertion of many connective tissues and would have important applications in tissue engineering.

Biomaterial scaffolds

Biomaterial scaffolds are an important component of tissue engineering that are used alone as a structural support for tissue growth or as a delivery platform for cells or biomolecules [112]. A variety of scaffold structures has been developed to suit different applications, including hydrogels, porous catheters, sponges, and nanofibers. These structures are derived from natural or synthetic materials. Natural materials often have high biocompatibility, recognition domains, and hydrophobicity and lack cellular interactions that can lead to poor cell reaction or poor integration with the host tissue. Therefore, a major focus of tissue engineering research is the design of bio-materials that provide information about cells and tissues. Inspired by mussel adhesion, scientists found that dopamine self-polymerized under alkaline conditions [63,65]. The reaction provides a universal coating for metals, polymers, and ceramics, regardless of their chemical and physical properties. In addition, this polymeric layer is rich in catechol groups and has been used to immobilize primary amines or thiol biomolecules via a simple dipping process. Wu et al. generated a 3D printed bio-

ceramic scaffold with a uniform self-assembled calcium phosphate/polydopamine nanolayer surface using biocompatibility, biodegradability, and the excellent photothermal effect of polydopamine (Fig. 7A) [122]. The designed bifunctional scaffolds with mussel-inspired nanostructures were used as a satisfactory controlled photothermal agent to effectively induce tumor cell death and inhibit tumor cell growth in mice. In addition, the prepared polydopamine-modified bioceramic scaffolds supported the attachment and proliferation of rabbit bone marrow mesenchymal stem cells (rBMSCs) and significantly promoted the formation of new bone tissue, even in response to a photothermal treatment.

Different materials, such as natural/synthetic polymers, carbon nanotubes, hydroxyapatite (HAp), and silicates, have been used to design and process nanocomposites to meet the diverse needs of tissue engineering [111,123–125]. Special attention has been given to the combination of biopolymers (i.e., proteins, polysaccharides, and glycosaminoglycans) with inorganic/ceramic fillers, which provide biomaterial composites with optimized properties [125]. The natural tissue interface is a continuous gradient structure; thus, versatile biological composites are needed to create suitable biomimetic engineered grafts for interfacial tissue engineering. Kaplan et al. used silk protein-based composites along with selective peptides and mineralized domains to mimic cartilage-to-bone conversion at the osteochondral interface. Gradient composites support tunable mineralization and mechanical properties corresponding to the spatial concentration gradients of mineralized domains (R5 peptides). The composite system showed a continuous change in composition, structure, and mechanical properties, as well as cell compatibility and biodegradability [124]. Panzavolta et al. developed a hybrid scaffold that consisted of a unique but integral layer capable of simulating different areas of cartilage and bone for osteochondral interface regeneration (Fig. 7B) [126]. The authors developed assemblies composed of a layer of gelatin with a layer containing different amounts of gelatin and hydroxyapatite nanocrystals and glued the layers together using a gelatin solution to form a multilayered scaffolds. The scaffolds exhibited high interconnected porosity and mechanical properties that varied with stent thickness, compressive stress, and modulus values of approximately 1 and 14 MPa.

Blood vessels play an important role in tissue engineering by serving as transport channels for nutrient and gas exchange. The successful function of these vessels is highly dependent on their ability to mimic the native arteries. However, their complex handling, controversial integrity, or uncontrollable cell location and orientation limit the currently available vascular prostheses [127]. Polymeric inverse opal films have been stretched into oval porous patterned substrates, and cells grew in a certain direction on these substrates [128,143]. However, the construction of three-

dimensional tubular inverse opal films, which have elliptical porous pattern surfaces, and their use as scaffolds in tissue engineering research has not been investigated. Thus, Zhao et al. proposed a new tubular scaffold with a specific surface microstructure that imitated a structural container (Fig. 7C) [127]. Tubular stents were constructed by rotationally expanding a three-dimensional tubular inverse opal film replicated from a colloidal crystal template in a capillary tube. Due to the ordered porous structure of inverse opal films, the expanded tubular scaffold had an elliptical patterned microstructure oriented circumferentially on its surface. These customized tubular scaffolds were effective in enabling endothelial cells to form an integrated, hollow tubular structure on their inner surface and induced smooth muscle cells to form a circumferential orientation on their outer surface (Fig. 7D). These features of our tubular scaffolds hold great promise for the construction of biomimetic vessels.

Biosensors

Biosensors are instruments that are sensitive to biological matter and converts their concentrations to electrical signals for detection and include immobilized bio-sensitive materials for identifying elements (including enzymes, antibodies, antigens, microorganisms, cells, tissues, nucleic acids, and other bioactive substances), suitable physical and chemical transducers (such as oxygen electrodes, phototubes, piezoelectric crystals), and signal amplification devices. Biosensors function as a receptor and a transducer [129].

SERS

Natural biological organisms with fine micro-/nanostructures have been used as biosensors, due to their low cost, easy availability, and biodegradability. Naturally occurring nanostructures with fine micro-papillae structures, such as cicada and butterfly wings, have been used for surface-enhanced Raman scattering (SERS) substrates [17,44]. *Graphium weiskei* butterfly wings have been confirmed to contain a nanoconical structure of chitin, which is a structural protein located in the purple and blue regions and has been used to create a biocompatible SERS platform [45,130]. Wood et al. used a SERS platform composed of gold-coated *G. weiskei* wings to detect hemozoin crystals in early circular lysate blood samples containing 0.0005 and 0.005% early ring-stage *P. falciparum*-infected RBCs [45]. The authors identified the key characteristic spectral markers of the malaria agent *P. falciparum* and detected early stages of parasitemia at levels ranging from 0.0005 to 0.005% in lysates from infected RBC samples, thus revealing the suitability of these substrates for biomedical applications of SERS. In addition, the naturally occurring wings with nanostructures have been utilized

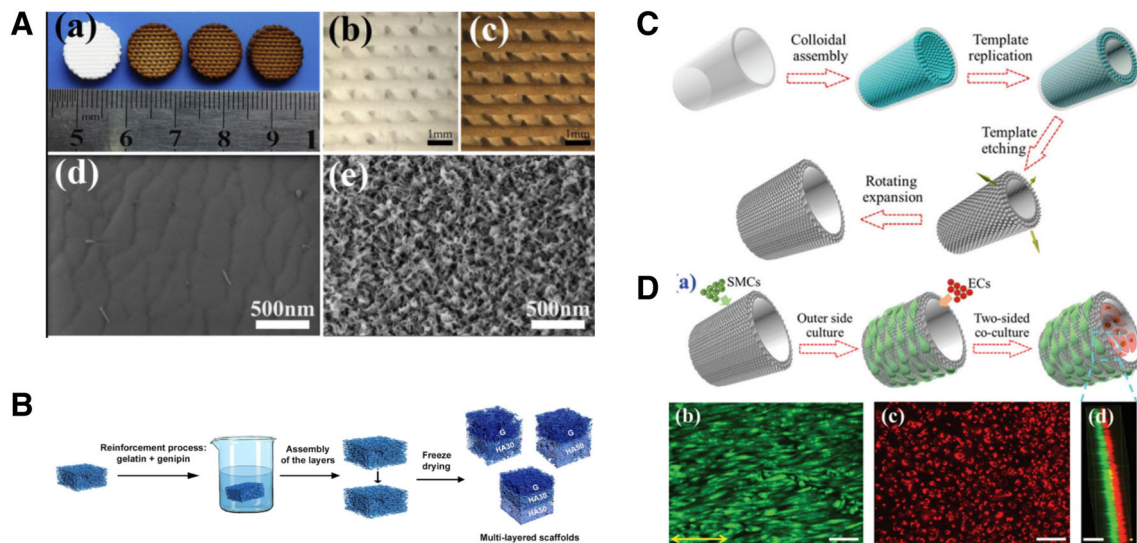


Fig. 7 **A** (a) Photographs of 3D printed pure bioceramics (BC), DOPA-BC (2 mg/mL), DOPA-BC (4 mg/mL), and DOPA-BC (6 mg/mL) scaffolds. Optical images of pure BC (b) and 4 mg/mL DOPA-BC (c) scaffolds from the top view. Scanning electron microscopy (SEM) images of pure BC (d), 2 mg/mL DOPA-BC (e), 4 mg/mL DOPA-BC (f), and 6 mg/mL DOPA-BC scaffolds. Reproduced with permission from [122]. Copyright 2016, Elsevier. **B** Schematic of the procedure utilized to assemble two- and three-layer scaffolds. Reproduced with permission from [126]. Copyright 2015, Wiley-VCH. **C** Schematic of the fabrication process for tubular scaffolds with circumferentially oriented ellipse inverse opal microstructures. Reproduced with permission

from [127]. Copyright 2016, The Royal Society of Chemistry. **D** (a) Schematic of the construction of the bioinspired vessels based on the expanded tubular inverse opals. (b, c) Fluorescence microscopy images of (b) A7r5 (green) cultured on the outer surface and (c) HUVECs (red) cultured on the inner surface of the scaffolds, scale bars for (b, c) and (d) represent 200 μm and 50 μm , respectively. Double-sided arrows indicate the circumferential direction. (d) Confocal image of a 3D reconstruction of the bioinspired vessel captured at a partial cross-section. Reproduced with permission from [127]. Copyright 2016, The Royal Society of Chemistry

as SERS substrate for biomarkers. Zhang et al. fabricated a stable and simple SERS-based readout assay to detect a significant tumor marker, carcinoembryonic antigen (CEA) [46]. The authors utilized Au-coated butterfly wings with a natural three-dimensional (3D) graded submicron structure rather than relying on aggregates of metal nanoparticles. The fabricated Au-coated butterfly wings showed excellent SERS performance and stability at a high temperature (80 °C) and long periods (6 months) at the submicron level. The authors used enzyme-linked immunosorbent assays (ELISA) to detect antibodies that can be replaced with chemically synthesized CEA aptamers, which could greatly simplify the entire assay.

Our group also has performed a series of studies on SERS based on bio-inspired materials. Plasma nanoparticles are commonly used as optical sensors in sensing applications, and the optical signal produced by the interaction of the analyte with the plasmonic nanoparticle is influenced by the surrounding physical structure in which the nanoparticle is located. Mu et al. presented a three-dimensional structure of inverse opal photonic crystal hydrogels to improve the Raman signal from plasma for protein and DNA analysis [Fig. 8A(a)] [131]. A SERS analysis of the composite protein was achieved by the hybridization of plasmonic nanoparticles and photonic crystals. This process favored the Raman

analysis by providing a high density of “hot spots” in a 3D array, as well as the additional enhancement of the local electromagnetic field at the edge of the PhC band and the periodic refractive index profile. Liu et al. conducted a multiplex bio-analysis using photonic crystals and SERS for dual coding, as shown in Fig. 8A(b) [132]. PC beads and SERS nanotags served as carriers and tags, respectively, for the sandwich detection of multiple antigens. In addition to the amplification capabilities of both encoding modes, the authors also showed that the quantitative analysis of multiple analytes displayed good stability, a low background, and high sensitivity. Meanwhile, these researchers also proposed an ultra-sensitive protein biosensor with a core-shell SERS nanotag as a marker and photonic crystal beads (PCBs) as a carrier [Fig. 8A(c)] [133]. Raman dyes (RDs) were embedded in the interface between the gold core and the silver shell in the bimetallic nanoparticles to form SERS nanotags. The sensitivity was significantly improved because the Raman signals enhanced by the coupling of core-shell structures, and the linear dynamic range (LDR) was prolonged due to the high surface area-to-volume ratio of PCBs. Overall, the fabricated SERS substrate displays a good stability and a low background and has great potential for applications in the detection of biomarkers.

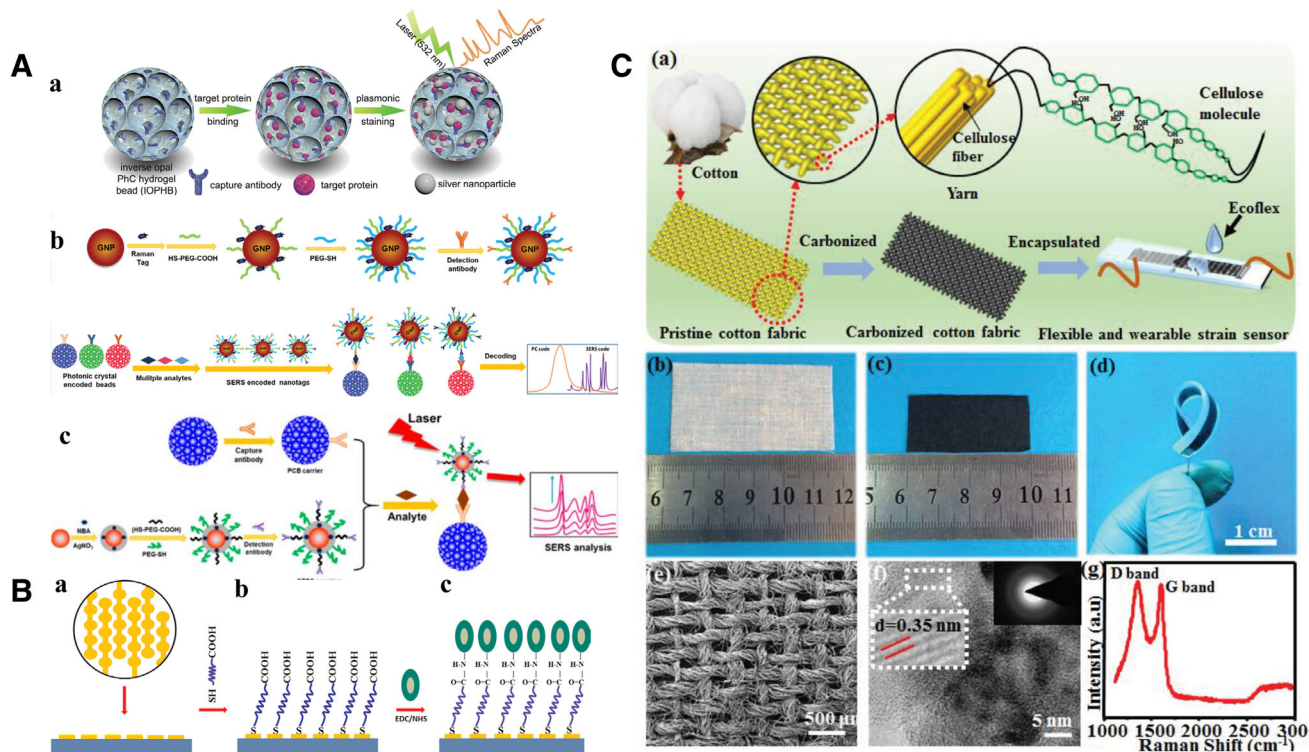


Fig. 8 **A** (a) Schematic of photonic-plasmonic hybrid IOPHB for the multiplex analysis of proteins based on their Raman fingerprints. IOPHBs were fabricated using self-assembled silica photonic crystal beads (PCBs) as templates. (b) Schematic of the SERS nanotag preparation and multiplex bioassays generated using photonic crystal beads and SERS nanotags. (c) Schematic of the protein detection process using SERS nanotags of Au@Ag NP and PCB. Reproduced with permission from [131,132]. Copyright 2015, Wiley-VCH, 2016, The

Royal Society of Chemistry. **B** OBPs immobilized on PEG-modified interdigitated electrodes. (a) Schematic of the interdigitated electrodes, (b) COOH-PEG-SH forms Au-S bonds with gold electrodes, and (c) BdorOBP2 forms covalent amino bonds with PEG-electrodes by EDC/NHS coupling. Reproduced with permission from [135]. Copyright 2014, Elsevier B.V. **C** Fabrication process and characterization of carbonized plain weave cotton fabric (CPCF). Reproduced with permission from [138]. Copyright 2016, Wiley-VCH

Gas sensor

In addition to the natural surface-based sensors, insects have a delicate sense of smell that allows them to sensitively and selectively detect thousands of chemical pheromones at very low concentrations through their remarkable olfactory system, which has been used to construct gas sensors [134,135]. For insects, the outstanding selectivity and sensitivity of the olfactory system is achieved by filters that discriminate between small soluble binding proteins and odorant receptors. These soluble binding proteins (mainly odor-binding proteins (OBPs)) are not only readily expressed and purified but are also highly stable to temperature, pH, solvents and proteases [136]. As one of the most important olfactory proteins, odorant-binding proteins (OBPs) from insects are the most promising candidates for producing biosensors to detect biochemical molecules in chemical ecology and other biotechnological applications. OBPs and peptide sequences derived from the insect OBPs (*Drosophila* and *Apis mellifera*) have been used to detect floral odors, alcohols and

explosives. Therefore, Liu et al. designed an olfactory biosensor to immobilize OBPs from oriental fruit fly to detect the semiochemicals (Fig. 8B) [135]. After successful isolation and purification, OBPs were immobilized with a specially designed polyethylene glycol (PEG) SH-PEG-COOH linkage to generate a robust sensor membrane, which sensitively detected isoamyl acetate, beta-ionone, benzaldehyde, and other compounds.

Electronic sensors

Natural biomaterial-derived carbon materials, such as carbonized filaments, are potential elements for the manufacture of low-cost, scalable, and environmentally friendly electronic components due to their abundance, renewability, and conductive properties [137,138]. Cotton is undoubtedly the dominant natural fiber used in our daily life for apparel and textiles. Plain cotton is one of the most popular cotton fabrics. It consists of warp yarns and weft yarns (each yarn consists of dozens of twisted cotton fibers) that are aligned to

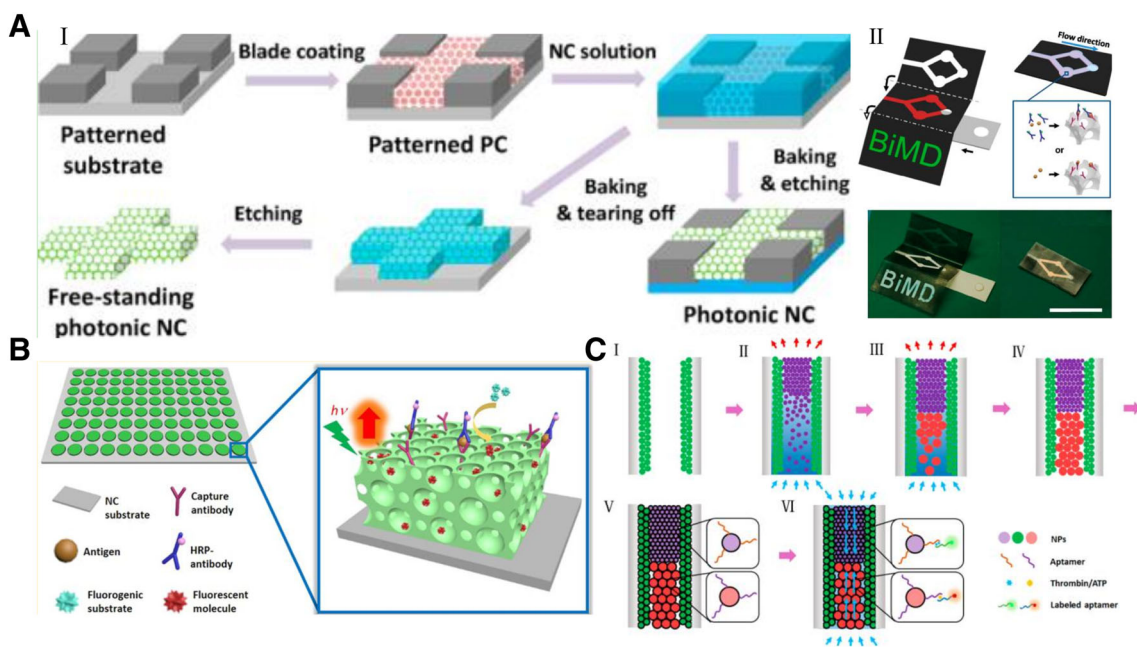


Fig. 9 **A** Schematic showing the procedure for fabricating the patterned photonic NC (I). Schematic and photographs showing the unfolded analytical device with photonic NC channels (red) for lateral-flow assays and label-free detection of analytes using the device (scale bar: 2 cm) (II). Reproduced with permission from [141]. Copyright 2016, American Chemical Society. **B** Schematic showing the pho-

tonic pseudopaper and fluorescence ELISA performed on the substrate. Reproduced with permission from [142]. Copyright 2017, American Chemical Society. **C** Schematic showing the procedure used to fabricate the opal capillary with multiple heterostructures for enhanced fluorescent aptamer-based assays. Reproduced with permission from [143]. Copyright 2017, American Chemical Society

form a simple cross-shaped pattern. Although natural cotton fibers are not electrically conductive, a simple heat treatment can convert them to highly conductive carbon fibers, while maintaining the original integrity and flexibility of the fibers [139]. Zhang et al. fabricated highly sensitive, wearable strain sensors based on commercial plain weave cotton fabric, which showed a large machinable strain range (> 140%), high sensitivity (strain of 0–80% and strain of 80–140%), unobtrusive drift, and long-term stability, while having the advantages of a low cost and a simple manufacturing process, and versatile applications (Fig. 8C) [138]. Likewise, Kim et al. reported a novel bio-piezoelectric nanogenerator (BPNG) that uses naturally rich, self-aligned cellulose fibers and an untreated onion skin (OS) as an effective piezoelectric material with ~ 2.8 pC/N of piezoelectric strength [140]. The prepared OSBPNG produces high-voltage electrical energy conversion efficiencies, which produced a maximum output voltage (approximately 106 V) when 6 cells were connected in series, instantly providing 73 combinations of LEDs. The OSBPNG was also very effective in promoting throat movements, such as coughing, alcohol consumption, and swallowing. Furthermore, it could be used for pacemakers and healthcare units and distinguishing voice signals, indicating the potential for speech recognition.

Microfluidics

In the field of biosensors, biochemical analyses comprise the majority of applications. Our group has long been engaged in biomedical engineering research, including bio-inspired materials, biosensors, and microfluidics. Gao and colleagues are mainly committed to biochemical analyses based on photonic crystals [141–143]. They fabricated a pseudopaper microfluidic chip based on patterned photonic nitrocellulose using self-assembled monodisperse silica nanoparticles as a template [141]. SiO₂ nanoparticles were used to form photonic crystals with well-arranged hexagonal structures in the micro-channels, thus resulting in nitrocellulose with complementary inverse opal structures (Fig. 9A). After lamination, a hollow channel that was partially filled with photon nitrocellulose was obtained to increase the fluorescence intensity for multiplex detection of human immunoglobulin G and two cancer biomarkers: carcinoembryonic antigen (CEA) and α -fetoprotein (AFP). In addition, the pseudopaper can be used for a highly sensitive fluorescent bio-analysis with enzyme-linked immunosorbent assays (ELISA) based on the fluorescence enhancement of photonic crystals (Fig. 9B) [142]. Due to the slow photon effect of the photonic structure, the fluorescence emission of the ELISA increased up to 57-fold without increasing assay time or complexity. As

the detection signal was significantly amplified, a simple smartphone camera was a sufficient detector for fast, on-site analysis. As proof of concept, a quantitative analysis of human IgG, with a limit of detection of 3.8 fg/mL, was below the limits of a conventional ELISA and paper-based ELISA.

In addition, the fluorescence enhancement of photonic crystal has also been used to generate analytical capillary devices for real-time detection. Gao et al. reported a method for producing opal capillaries with multiple heterostructures for aptamer-based assays inspired by plant transpiration (Fig. 9C) [143]. During the manufacturing process, monodisperse SiO₂ nanoparticles (NPs) self-assemble in glass capillaries and solvents are gradually evaporated from the top of the capillaries. Multiple heterostructures are easily prepared inside the capillaries by simply changing the colloidal solution through the capillaries. Polydopamine was coated on the surface of the silica nanoparticles with immobilized aminomethyl-modified aptamers for the fluorescence detection of adenosine triphosphate (ATP) and thrombin. Due to the fluorescence-enhancing effect of photonic heterostructures, the fluorescence signal for detection is amplified up to 40-fold. The limit of detection for ATP was 32 μM, and the limit of detection for thrombin was 8.1 nM.

Conclusion and perspective

In recent years, multiple types of nature sourced substrates have been utilized or duplicated for biomedical applications, in this review we have presented a comprehensive summary of recent progress on bio-sourced or bio-inspired materials and structures and their applications in biomedical engineering. Because of the deeply theoretical research and technological innovations, biological materials currently bear significant value in an extremely wide range of areas, including physical, chemical, biological, engineering, and medical fields. Despite the many exciting and compelling developments, there remain challenges that pose a gap between academic proof-of-concept studies and practical techniques for addressing real-world problems. For example, detection direct on bio-sourced materials still remains great challenges since individual difference of same organisms, also here is still room for improvement of the existing fabrication methods.

In summary, we anticipate that those natural substrates originating from natural will have important applications in tissue engineering. As well as a natural scaffold for 3D tissue culture for study the in-vivo cell morphology and functions, further future research is still required to optimize these models to enable their introduction to the field of tissue engineering as the natural biocompatible and biodegradable scaffolds. Moreover, the natural ordered structure itself is a

promising alternative to POCT and may assist patients in challenging and underdeveloped areas.

Acknowledgements We gratefully acknowledge financial support from the Innovative and Entrepreneurial Talent Recruitment Program of Jiangsu Province, the National Natural Science Foundation of China (21405014, 21635001, 21627806 and 21501026), Key Research and Development Plan of Jiangsu Province BE2016002, the Project of Special Funds of Jiangsu Province for the Transformation of Scientific and Technological Achievements (BA2015067), the 111 Project (B17011, Ministry of Education of China), and the Natural Science Foundation of Jiangsu Province (BK20140626 and BK20140619). China Postdoctoral Science Foundation funded Project (2017M621597). The Fundamental Research Funds for the Central Universities (2242018R20011).

Author contributions ZG developed the idea; AE, ZH and BG drafted the manuscript; JC, ES, DZ, SL, HX, and HL revised the manuscript. All authors reviewed the content and have given approval to the final version of the manuscript.

Compliance with ethical standards

Conflict of interest The authors declare no competing financial interests.

References

- Roth RR (1983) The foundation of bionics. *Perspect Biol Med* 26(2):229–242
- Wahl D (2006) Bionics vs. biomimicry: from control of nature to sustainable participation in nature. In: *Design and nature III: comparing design in nature with science and engineering*, vol 87, pp 289–298
- Bar-Cohen Y (2012) Nature as a model for mimicking and inspiration of new technologies. *Int J Aeronaut Space Sci* 13(1):1–13
- Wang Z, Hang G, Li J, Wang Y, Xiao K (2008) A micro-robot fish with embedded SMA wire actuated flexible biomimetic fin. *Sens Actuators A* 144(2):354–360
- Rumelhart DE (1989) Toward a microstructural account of human reasoning. In: Vosniadou S, Ortony A (eds) *Similarity and analogical reasoning*. Cambridge University Press, New York, p 298
- Liu K, Jiang L (2011) Multifunctional integration: from biological to bio-inspired materials. *ACS Nano* 5(9):6786–6790
- Cheung T (2006) From the organism of a body to the body of an organism: occurrence and meaning of the word ‘organism’ from the seventeenth to the nineteenth centuries. *Br J Hist Sci* 39(3):319–339
- Mora C, Tittensor DP, Adl S, Simpson AGB, Worm B (2011) How many species are there on earth and in the ocean? *PLoS Biol* 9(8):e1001127
- Ramos M, Lobo J, Esteban M (2001) Ten years inventorying the Iberian fauna: results and perspectives. *Biodivers Conserv* 10(1):19–28
- Liu K, Yao X, Jiang L (2010) Recent developments in bio-inspired special wettability. *Chem Soc Rev* 39(8):3240–3255
- Liu K, Jiang L (2011) Bio-inspired design of multiscale structures for function integration. *Nano Today* 6(2):155–175
- Gao X, Yan X, Yao X, Xu L, Zhang K, Zhang J, Yang B, Jiang L (2007) The dry-style antifogging properties of mosquito compound eyes and artificial analogues prepared by soft lithography. *Adv Mater* 19(17):2213–2217

13. Ko D, Tumbleston JR, Henderson KJ, Euliss LE, DeSimone JM, Lopez R, Samulski ET (2011) Biomimetic microlens array with antireflective "moth-eye" surface. *Soft Matter* 7:6404–6407
14. Boden SA, Bagnall DM (2010) Optimization of moth-eye antireflection schemes for silicon solar cells. *Prog Photovolt Res Appl* 18(3):195–203
15. Zhang G, Zhang J, Xie G, Liu Z, Shao H (2006) Cicada wings: a stamp from nature for nanoimprint lithography. *Small* 2(12):1440–1443
16. Huang Y-F, Jen Y-J, Chen L-C, Chen K-H, Chattopadhyay S (2015) Design for approaching cicada-wing reflectance in low- and high-index biomimetic nanostructures. *ACS Nano* 9(1):301–311
17. Jiwei Q, Yudong L, Ming Y, Qiang W, Zongqiang C, Wudeng W, Wenqiang L, Xuanyi Y, Jingjun X, Qian S (2013) Large-area high-performance SERS substrates with deep controllable sub-10-nm gap structure fabricated by depositing Au film on the cicada wing. *Nanoscale Res Lett* 8(1):437
18. Yao X, Chen Q, Xu L, Li Q, Song Y, Gao X, Quéré D, Jiang L (2010) Bioinspired ribbed nanoneedles with robust superhydrophobicity. *Adv Funct Mater* 20(4):656–662
19. Hu DL, Chan B, Bush JW (2003) The hydrodynamics of water strider locomotion. *Nature* 424(6949):663–666
20. Gao X, Jiang L (2004) Biophysics: water-repellent legs of water striders. *Nature* 432(7013):36–36
21. Shi F, Niu J, Liu J, Liu F, Wang Z, Feng XQ, Zhang X (2007) Towards understanding why a superhydrophobic coating is needed by water striders. *Adv Mater* 19(17):2257–2261
22. Parker AR, Lawrence CR (2001) Water capture by a desert beetle. *Nature* 414(6859):33–34
23. Zeng X, Qian L, Yuan X, Zhou C, Li Z, Cheng J, Xu S, Wang S, Pi P, Wen X (2016) Inspired by stenocara beetles: from water collection to high-efficiency water-in-oil emulsion separation. *ACS Nano* 11(1):760–769
24. Usherwood JR, Lehmann F-O (2008) Phasing of dragonfly wings can improve aerodynamic efficiency by removing swirl. *J R Soc Interface* 5(28):1303–1307
25. Soms C, Luttes M (1985) Dragonfly flight: novel uses of unsteady separated flows. *Science* 228:1326–1330
26. Dudley R (2000) The biomechanics of insect flight: form, function, evolution. Princeton University Press, Princeton, p 476
27. Okamoto M, Yasuda K, Azuma A (1996) Aerodynamic characteristics of the wings and body of a dragonfly. *J Exp Biol* 199(2):281–294
28. Nguyen SHT, Webb HK, Hasan J, Tobin MJ, Crawford RJ, Lvanova EP (2013) Dual role of outer epicuticular lipids in determining the wettability of dragonfly wings. *Colloids Surf B* 106:126–134
29. Nakata T, Liu H, Tanaka Y, Nishihashi N, Wang X, Sato A (2011) Aerodynamics of a bio-inspired flexible flapping-wing micro air vehicle. *Bioinspir Biomim* 6(4):045002
30. Chung K, Yu S, Heo CJ, Shim JW, Yang SM, Han MG, Lee HS, Jin Y, Lee SY, Park N (2012) Flexible, angle-independent, structural color reflectors inspired by morpho butterfly wings. *Adv Mater* 24(18):2375–2379
31. Kinoshita S, Yoshioka S (2005) Structural colors in nature: the role of regularity and irregularity in the structure. *ChemPhysChem* 6(8):1442–1459
32. Peng W, Zhu S, Zhang W, Yang Q, Zhang D, Chen Z (2014) Spectral selectivity of 3D magnetophotonic crystal film fabricated from single butterfly wing scales. *Nanoscale* 6(11):6133–6140
33. Li Q, Zeng Q, Shi L, Zhang X, Zhang KQ (2016) Bio-inspired sensors based on photonic structures of Morpho butterfly wings: a review. *J Mater Chem C* 4(9):1752–1763
34. Bixler GD, Bhushan B (2012) Bioinspired rice leaf and butterfly wing surface structures combining shark skin and lotus effects. *Soft Matter* 8(44):11271–11284
35. Zheng Y, Gao X, Jiang L (2007) Directional adhesion of superhydrophobic butterfly wings. *Soft Matter* 3(2):178–182
36. Potyrailo RA, Bonam RK, Hartley JG, Starkey TA, Vukusic P, Vasudev M, Bunning T, Naik RR, Tang Z, Palacios MA (2015) Towards outperforming conventional sensor arrays with fabricated individual photonic vapour sensors inspired by Morpho butterflies. *Nat Commun* 6:7959
37. Zhu X, Zhang H, Wu J (2014) Chemiresistive ionogel sensor array for the detection and discrimination of volatile organic vapor. *Sens Actuators B Chem* 202:105–113
38. Potyrailo RA, Starkey TA, Vukusic P, Ghiradella H, Vasudev M, Bunning T, Naik RR, Tang Z, Larsen M, Deng T (2013) Discovery of the surface polarity gradient on iridescent Morpho butterfly scales reveals a mechanism of their selective vapor response. *Proc Nat Acad Sci USA* 110(39):15567–15572
39. John S (1987) Strong localization of photons in certain disordered dielectric superlattices. *Phys Rev Lett* 58(23):2486–2489
40. Lu T, Zhu S, Ma J, Lin J, Wang W, Pan H, Tian F, Zhang W, Zhang D (2015) Bioinspired thermoresponsive photonic polymers with hierarchical structures and their unique properties. *Macromol Rapid Commun* 36(19):1722–1728
41. Xu D, Yu H, Xu Q, Xu G, Wang K (2015) Thermoresponsive photonic crystal: synergistic effect of poly(*N*-isopropylacrylamide)-*co*-acrylic acid and morpho butterfly wing. *ACS Appl Mater Interfaces* 7(16):8750–8756
42. Pris AD, Utturkar Y, Surman C, Morris WG, Vert A, Zalyubovskiy S, Deng T, Ghiradella HT, Potyrailo RA (2012) Towards high-speed imaging of infrared photons with bio-inspired nanoarchitectures. *Nat Photonics* 6(3):195–200
43. Zhang F, Shen Q, Shi X, Li S, Wang W, Luo Z, He G, Zhang P, Tao P, Song C (2015) Infrared detection based on localized modification of Morpho butterfly wings. *Adv Mater* 27(6):1077–1082
44. Mu Z, Zhao X, Xie Z, Zhao Y, Zhong Q, Bo L, Gu Z (2013) In situ synthesis of gold nanoparticles (AuNPs) in butterfly wings for surface enhanced Raman spectroscopy (SERS). *J Mater Chem B* 1(11):1607–1613
45. Garrett NL, Sekine R, Dixon MW, Tilley L, Bambery KR, Wood BR (2015) Bio-sensing with butterfly wings: naturally occurring nano-structures for SERS-based malaria parasite detection. *Phys Chem Chem Phys* 17(33):21164–21168
46. Song G, Zhou H, Gu J, Liu Q, Zhang W, Su H, Su Y, Yao Q, Zhang D (2017) Tumor marker detection using surface enhanced Raman spectroscopy on 3D Au butterfly wings. *J Mater Chem B* 5(8):1594–1600
47. Badge I, Stark AY, Paoloni EL, Niewiarowski PH, Dhinojwala A (2014) The role of surface chemistry in adhesion and wetting of gecko toe pads. *Sci Rep* 4(6643):6643–6643
48. Peng J, Yu P, Zeng S, Liu X, Chen J, Xu W (2010) Application of click chemistry in the fabrication of cactus-like hierarchical particulates for sticky superhydrophobic surfaces. *J Phys Chem C* 114(13):5926–5931
49. Liu K, Du J, Wu J, Jiang L (2012) Superhydrophobic gecko feet with high adhesive forces towards water and their bio-inspired materials. *Nanoscale* 4(3):768–772
50. Li Z, Du R (2013) Design and analysis of a bio-inspired wire-driven multi-section flexible robot. *Int J Adv Rob Syst* 10(4):209–220
51. Hirose S, Mori M (2004) Biologically inspired snake-like robots. In: IEEE international conference on robotics and biomimetics, 2004, ROBIO 2004. IEEE, pp 1–7

52. Crespi A, Ijspeert AJ (2008) Online optimization of swimming and crawling in an amphibious snake robot. *IEEE Trans Rob* 24(1):75–87
53. Meyers MA, Lin AYM, Seki Y, Chen PY, Kad BK, Bodde S (2006) Structural biological composites: an overview. *JOM* 58(7):35–41
54. Sachs C, Fabritius H, Raabe D (2006) Experimental investigation of the elastic-plastic deformation of mineralized lobster cuticle by digital image correlation. *J Struct Biol* 155(3):409–425
55. Rhee H, Horstemeyer MF, Hwang Y, Lim H, Kadiri HE, Trim W (2009) A study on the structure and mechanical behavior of the *Terrapene carolina* carapace: a pathway to design bio-inspired synthetic composites. *Mater Sci Eng C* 29(8):2333–2339
56. Thorbjarnarson J (1999) Crocodile tears and skins: international trade, economic constraints, and limits to the sustainable use of crocodilians. *Conserv Biol* 13(3):465–470
57. Buthelezi S, Southway C, Govinden U, Bodenstern J, Du TK (2012) An investigation of the antimicrobial and anti-inflammatory activities of crocodile oil. *J Ethnopharmacol* 143(1):325–330
58. Qin Z, Pugno NM, Buehler MJ (2014) Mechanics of fragmentation of crocodile skin and other thin films. *Sci Rep* 4(21):4966
59. Milinkovitch MC, Zwicker M (2013) Crocodile head scales are not developmental units but emerge from physical cracking. *Science* 339(6115):78–81
60. Yao HB, Fang HY, Wang XH, Yu SH (2011) Hierarchical assembly of micro-/nano-building blocks: bio-inspired rigid structural functional materials. *Chem Soc Rev* 40(7):3764–3785
61. Meyers MA, Lin AYM, Chen PY, Muyco J (2008) Mechanical strength of abalone nacre: role of the soft organic layer. *J Mech Behav Biomed Mater* 1(1):76–85
62. Barthelat F, Tang H, Zavattieri PD, Li CM, Espinosa HD (2007) On the mechanics of mother-of-pearl: a key feature in the material hierarchical structure. *J Mech Phys Solids* 55(2):306–337
63. Lee H, Dellatore SM, Miller WM, Messersmith PB (2007) Mussel-inspired surface chemistry for multifunctional coatings. *Science* 318(5849):426
64. Kang SM, You I, Cho WK, Shon HK, Lee TG, Choi IS, Karp JM, Lee H (2010) One-step modification of superhydrophobic surfaces by a mussel-inspired polymer coating. *Angew Chem Int Ed* 49(49):9401–9404
65. Ryu J, Ku SH, Lee H, Park CB (2010) Mussel-inspired polydopamine coating as a universal route to hydroxyapatite crystallization. *Adv Funct Mater* 20(13):2132–2139
66. Rui D, Zhang J, Du X, Yao X, Kunihiko K (2009) Properties of collagen from skin, scale and bone of carp (*Cyprinus carpio*). *Food Chem* 112(3):702–706
67. Zylberberg L, Bonaventure J, Cohen-Solal L, Hartmann DJ, Bereiterhahn J (1992) Organization and characterization of fibrillar collagen in fish scales in situ and in vitro. *China J Chin Mater Med* 103(15):273–285
68. Papastamatiou YP, Cartamil DP, Lowe CG, Meyer CG, Wetherbee BM, Holland KN (2011) Scales of orientation, directed walks and movement path structure in sharks. *J Anim Ecol* 80(4):864–874
69. Zhu D, Ortega CF, Motamedi R, Szewciw L, Vernerey F, Barthelat F (2012) Structure and mechanical performance of a “modern” fish scale. *Adv Eng Mater* 14(4):185–194
70. Knackstedt MA, Arns CH, Senden TJ, Gross K (2006) Structure and properties of clinical coralline implants measured via 3D imaging and analysis. *Biomaterials* 27(13):2776–2786
71. Wang Y, Tao S, An Y, Wu S, Meng C (2013) Bio-inspired high performance electrochemical supercapacitors based on conducting polymer modified coral-like monolithic carbon. *J Mater Chem A* 1(31):8876–8887
72. Yeom SW, Oh IK (2009) A biomimetic jellyfish robot based on ionic polymer metal composite actuators. *Smart Mater Struct* 18(8):085002
73. Najem J, Sarles SA, Akle B, Leo DJ (2012) Biomimetic jellyfish-inspired underwater vehicle actuated by ionic polymer metal composite actuators. *Smart Mater Struct* 21(9):299–312
74. Zi J, Yu X, Li Y, Hu X, Xu C, Wang X, Liu X, Fu R (2003) Coloration strategies in peacock feathers. *Proc Natl Acad Sci USA* 100(22):12576–12578
75. Han J, Su H, Zhang C, Dong Q, Zhang W, Zhang D (2008) Embedment of ZnO nanoparticles in the natural photonic crystals within peacock feathers. *Nanotechnology* 19(36):365602
76. Jin Y, Yuan H, Lan J-L, Yu Y, Lin Y-H, Yang X (2017) Bio-inspired spider-web-like membranes with a hierarchical structure for high performance lithium/sodium ion battery electrodes: the case of 3D freestanding and binder-free bismuth/CNF anodes. *Nanoscale* 9(35):13298–13304
77. Sahni V, Blackledge TA, Dhinojwala A (2010) Viscoelastic solids explain spider web stickiness. *Nat Commun* 1:19
78. Ko FK, Jovicic J (2004) Modeling of mechanical properties and structural design of spider web. *Biomacromolecules* 5(3):780–785
79. Barthlott W, Neinhuis C (1997) Purity of the sacred lotus, or escape from contamination in biological surfaces. *Planta* 202(1):1–8
80. Feng L, Zhang Y, Xi J, Zhu Y, Wang N, Xia F, Jiang L (2008) Petal effect: a superhydrophobic state with high adhesive force. *Langmuir* 24(8):4114–4119
81. Darmanin T, Bombera R, Colpo P, Valsesia A, Laugier JP, Rossi F, Guittard F (2017) Bioinspired rose-petal-like substrates generated by electropolymerization on micropatterned gold substrates. *Chempluschem* 82(3):352–357
82. Feng L, Zhang Y, Xi J, Zhu Y, Wang N, Xia F, Jiang L (2008) Petal effect: a superhydrophobic state with high adhesive force. *Langmuir ACS J Surf Colloids* 24(8):4114–4119
83. Lai Y, Gao X, Zhuang H, Huang J, Lin C, Jiang L (2009) Designing superhydrophobic porous nanostructures with tunable water adhesion. *Adv Mater* 21(37):3799–3803
84. Bixler GD, Bhushan B (2012) Bioinspired rice leaf and butterfly wing surface structures combining shark skin and lotus effects. *Soft Matter* 8(44):11271–11284
85. Wu H, Zhang R, Sun Y, Lin D, Sun Z, Pan W, Downs P (2008) Biomimetic nanofiber patterns with controlled wettability. *Soft Matter* 4(12):2429–2433
86. Kang SM, Lee C, Kim HN, Lee BJ, Lee JE, Kwak MK, Suh KY (2013) Directional oil sliding surfaces with hierarchical anisotropic groove microstructures. *Adv Mater* 25(40):5756–5761
87. Bohn HF, Federle W (2004) From the cover: insect aquaplaning: *Nepenthes pitcher* plants capture prey with the peristome, a fully wettable water-lubricated anisotropic surface. *Proc Natl Acad Sci USA* 101(39):14138–14143
88. Chen H, Zhang P, Zhang L, Liu H, Jiang Y, Zhang D, Han Z, Jiang L (2016) Continuous directional water transport on the peristome surface of *Nepenthes alata*. *Nature* 532(7597):85–89
89. Chen H, Zhang L, Zhang P, Zhang D, Han Z, Jiang L (2017) A novel bioinspired continuous unidirectional liquid spreading surface structure from the peristome surface of *Nepenthes alata*. *Small* 13(4):1601676
90. Tan T, Rahbar N, Allameh SM, Kwofie S, Dissmore D, Ghavami K, Soboyejo WO (2011) Mechanical properties of functionally graded hierarchical bamboo structures. *Acta Biomater* 7(10):3796–3803
91. Tanaka A, Zhu Q, Tan H, Horiba H, Ohnuki K, Mori Y, Yamauchi R, Ishikawa H, Iwamoto A, Kawahara H (2014) Biological activities and phytochemical profiles of extracts from different parts of bamboo (*Phyllostachys pubescens*). *Molecules* 19(6):8238–8260

92. Tian WQ, Gao QM, Tan Y, Yang K, Zhu LH, Yang CX, Zhang H (2015) Bio-inspired beehive-like hierarchical nanoporous carbon derived from bamboo-based industrial by-product as a high performance supercapacitor electrode material. *J Mater Chem A* 3(10):5656–5664
93. Tian WQ, Gao QM, Tan Y, Yang K, Zhu LH, Yang CX, Zhang H (2015) Bio-inspired beehive-like hierarchical nanoporous carbon derived from bamboo-based industrial by-product as a high performance supercapacitor electrode material. *J Mater Chem A* 3(10):5656–5664
94. Sayler GS, Ripp S (2000) Field applications of genetically engineered microorganisms for bioremediation processes. *Curr Opin Biotechnol* 11(3):286–289
95. Idil N, Mattiasson B (2017) Imprinting of microorganisms for biosensor applications. *Sensors* 17(4):708
96. Yousuf A, Sannino F, Addorisio V, Pirozzi D (2010) Microbial conversion of olive oil mill wastewaters into lipids suitable for biodiesel production. *J Agric Food Chem* 58(15):8630–8635
97. Fan L, Song Y (2016) Overview on electricigens for microbial fuel cell. *Open Biotechnol J* 10(1):398–406
98. Veith B, Herzberg C, Steckel S, Feesche J, Maurer KH, Ehrenreich P, Bäumer S, Henne A, Liesegang H, Merkl R (2004) The complete genome sequence of *Bacillus licheniformis* DSM13, an organism with great industrial potential. *J Mol Microbiol Biotechnol* 7(4):204–211
99. Leroy F, De Vuyst L (2004) Lactic acid bacteria as functional starter cultures for the food fermentation industry. *Trends Food Sci Technol* 15(2):67–78
100. Dai X, Tian Y, Li J, Su X, Wang X, Zhao S, Liu L, Luo Y, Liu D, Zheng H (2015) Metatranscriptomic analyses of plant cell wall polysaccharide degradation by microorganisms in the cow rumen. *Appl Environ Microbiol* 81(4):1375–1386
101. Stoll ZA, Forrester C, Ren ZJ, Xu P (2015) Shale gas produced water treatment using innovative microbial capacitive desalination cell. *J Hazard Mater* 283:847–855
102. Mandal D, Bolander ME, Mukhopadhyay D, Sarkar G, Mukherjee P (2006) The use of microorganisms for the formation of metal nanoparticles and their application. *Appl Microbiol Biotechnol* 69(5):485–492
103. Ehrlich H, Motylenko M, Sundareshwar PV, Ereskovsky A, Zgłobicka I, Noga T, Płociński T, Tsurkan MV, Wyroba E, Suski S (2016) Multiphase biomineralization: enigmatic invasive siliceous diatoms produce crystalline calcite. *Adv Funct Mater* 26(15):2503–2510
104. Li Q, Gadd GM (2017) Biosynthesis of copper carbonate nanoparticles by ureolytic fungi. *Appl Microbiol Biotechnol* 101(19):7397–7407
105. Xia A, Jacob A, Tabassum MR, Herrmann C, Murphy JD (2016) Production of hydrogen, ethanol and volatile fatty acids through co-fermentation of macro-and micro-algae. *Bioresour Technol* 205:118–125
106. Xia A, Cheng J, Song W, Su H, Ding L, Lin R, Lu H, Liu J, Zhou J, Cen K (2015) Fermentative hydrogen production using algal biomass as feedstock. *Renew Sustain Energy Rev* 51:209–230
107. Ike A, Toda N, Tsuji N, Hirata K, Miyamoto K (1997) Hydrogen photoproduction from CO₂-fixing microalgal biomass: application of halotolerant photosynthetic bacteria. *J Ferment Bioeng* 84(6):606–609
108. Ren L, Ahn Y, Logan BE (2014) A two-stage microbial fuel cell and anaerobic fluidized bed membrane bioreactor (MFC-AFMBR) system for effective domestic wastewater treatment. *Environ Sci Technol* 48(7):4199–4206
109. Feng Y, He W, Liu J, Wang X, Qu Y, Ren N (2014) A horizontal plug flow and stackable pilot microbial fuel cell for municipal wastewater treatment. *Bioresour Technol* 156:132–138
110. Armentano I, Dottori M, Fortunati E, Mattioli S, Kenny J (2010) Biodegradable polymer matrix nanocomposites for tissue engineering: a review. *Polym Degrad Stab* 95(11):2126–2146
111. Jayakumar R, Prabakaran M, Nair S, Tamura H (2010) Novel chitin and chitosan nanofibers in biomedical applications. *Biotechnol Adv* 28(1):142–150
112. O'Brien FJ (2011) Biomaterials & scaffolds for tissue engineering. *Mater Today* 14(3):88–95
113. Lutolf MP, Hubbell JA (2005) Synthetic biomaterials as instructive extracellular microenvironments for morphogenesis in tissue engineering. *Nat Biotechnol* 23(1):47–55
114. Lee MK, Rich MH, Lee J, Kong H (2015) A bio-inspired, microchanneled hydrogel with controlled spacing of cell adhesion ligands regulates 3D spatial organization of cells and tissue. *Biomaterials* 58:26–34
115. Lee MK, Rich MH, Baek K, Lee J, Kong H (2015) Bioinspired tuning of hydrogel permeability-rigidity dependency for 3D cell culture. *Sci Rep* 5:8948
116. Tibbitt MW, Anseth KS (2009) Hydrogels as extracellular matrix mimics for 3D cell culture. *Biotechnol Bioeng* 103(4):655–663
117. Roy KJ, Smith S (1971) Sedimentation and coral reef development in turbid water: Fanning Lagoon. *Pac Sci* 25(2):234–248
118. Corson F (2010) Fluctuations and redundancy in optimal transport networks. *Phys Rev Lett* 104(4):048703
119. Li J, Wei J, Liu Y, Liu B, Liu T, Jiang Y, Ding L, Liu C (2017) A microfluidic design to provide a stable and uniform in vitro microenvironment for cell culture inspired by the redundancy characteristic of leaf areoles. *Lab Chip* 17(22):3921–3933
120. Lu J, Zheng F, Cheng Y, Ding H, Zhao Y, Gu Z (2014) Hybrid inverse opals for regulating cell adhesion and orientation. *Nanoscale* 6(18):10650–10656
121. Lu J, Zou X, Zhao Z, Mu Z, Zhao Y, Gu Z (2015) Cell orientation gradients on an inverse opal substrate. *ACS Appl Mater Interfaces* 7(19):10091
122. Ma H, Luo J, Sun Z, Xia L, Shi M, Liu M, Chang J, Wu C (2016) 3D printing of biomaterials with mussel-inspired nanostructures for tumor therapy and tissue regeneration. *Biomaterials* 111:138–148
123. Pina S, Oliveira JM, Reis RL (2015) Natural-based nanocomposites for bone tissue engineering and regenerative medicine: a review. *Adv Mater* 27(7):1143–1169
124. Wang X, Kim HJ, Wong C, Vepari C, Matsumoto A, Kaplan DL (2006) Fibrous proteins and tissue engineering. *Mater Today* 9(12):44–53
125. Swetha M, Sahithi K, Moorthi A, Srinivasan N, Ramasamy K, Selvamurugan N (2010) Biocomposites containing natural polymers and hydroxyapatite for bone tissue engineering. *Int J Biol Macromol* 47(1):1–4
126. Amadori S, Torricelli P, Panzavolta S, Parrilli A, Fini M, Bigi A (2015) Multi-layered scaffolds for osteochondral tissue engineering: in vitro response of co-cultured human mesenchymal stem cells. *Macromol Biosci* 15(11):1535–1545
127. Zhao Z, Wang J, Lu J, Yu Y, Fu F, Wang H, Liu Y, Zhao Y, Gu Z (2016) Tubular inverse opal scaffolds for biomimetic vessels. *Nanoscale* 8(28):13574–13580
128. Heyligers JMM, Arts CHP, Verhagen HJM, Groot PGD, Moll FL (2005) Improving small-diameter vascular grafts: from the application of an endothelial cell lining to the construction of a tissue-engineered blood vessel. *Ann Vasc Surg* 19(3):448–456
129. Turner AP (2000) Biosensors-sense and sensitivity. *Science* 290(5495):1315–1317
130. Garrett NL, Vukusic P, Ogrin F, Sirotkin E, Winlove CP, Moger J (2009) Spectroscopy on the wing: naturally inspired SERS substrates for biochemical analysis. *J Biophotonics* 2(3):157–166

131. Mu Z, Zhao X, Huang Y, Lu M, Gu Z (2015) Plasmonic staining: photonic crystal hydrogel enhanced plasmonic staining for multiplexed protein analysis. *Small* 11(45):6036–6043
132. Liu B, Zhao X, Jiang W, Fu D, Gu Z (2016) Multiplex bioassays encoded by photonic crystal beads and SERS nanotags. *Nanoscale* 8(40):17465–17471
133. Liu B, Ni H, Zhang D, Wang D, Fu D, Chen H, Gu Z, Zhao X (2017) Ultrasensitive detection of protein with wide linear dynamic range based on core–shell SERS nanotags and photonic crystal beads. *ACS Sens* 2(7):1035–1043
134. Ishida H, Suetsugu KI, Nakamoto T, Moriizumi T (1994) Study of autonomous mobile sensing system for localization of odor source using gas sensors and anemometric sensors. *Sens Actuators A* 45(2):153–157
135. Lu Y, Yao Y, Zhang Q, Zhang D, Zhuang S, Li H, Liu Q (2015) Olfactory biosensor for insect semiochemicals analysis by impedance sensing of odorant-binding proteins on interdigitated electrodes. *Biosens Bioelectron* 67:662–669
136. Sankaran S, Khot LR, Panigrahi S (2012) Biology and applications of olfactory sensing system: a review. *Sens Actuators B Chem* 171:1–17
137. Wang C, Li X, Gao E, Jian M, Xia K, Wang Q, Xu Z, Ren T, Zhang Y (2016) Carbonized silk fabric for ultrastretchable, highly sensitive, and wearable strain sensors. *Adv Mater* 28(31):6640–6648
138. Zhang M, Wang C, Wang H, Jian M, Hao X, Zhang Y (2017) Carbonized cotton fabric for high-performance wearable strain sensors. *Adv Funct Mater* 27(2):1604795
139. Liu H, Zhang Y, Li R, Sun X, Désilets S, Abou-Rachid H, Jaidann M, Lussier L-S (2010) Structural and morphological control of aligned nitrogen-doped carbon nanotubes. *Carbon* 48(5):1498–1507
140. Maiti S, Karan SK, Lee J, Mishra AK, Khatua BB, Kim JK (2017) Bio-waste onion skin as an innovative nature-driven piezoelectric material with high energy conversion efficiency. *Nano Energy* 42:282–293
141. Gao B, Hong L, Gu Z (2016) Patterned photonic nitrocellulose for pseudo-paper microfluidics. *Anal Chem* 88(10):5424–5429
142. Chi J, Gao B, Sun M, Zhang F, Su E, Liu H, Gu Z (2017) Patterned photonic nitrocellulose for pseudopaper ELISA. *Anal Chem* 89(14):7727–7733
143. Gao B, Tang L, Zhang D, Xie Z, Su E, Liu H, Gu Z (2017) Transpiration-inspired fabrication of opal capillary with multiple heterostructures for multiplex aptamer-based fluorescent assays. *ACS Appl Mater Interfaces* 9(38):32577–32582